Title
MOLECULAR BEAM STUDIES OF SCANDIUM MONOFLUORIDE.

Author
Green, David W.

Publication Date
1968

UCRL-17961

Cy.2

University of California

Ernest O. Lawrence Radiation Laboratory

MOLECULAR BEAM STUDIES OF SCANDIUM MONOFLUORIDE

David W. Green
(Ph. D. Thesis Part I)

January 1968

DISCLAIMER

UCRL-17961

UNIVERSITY OF CALIFORNIA

Lawrence Radiation Laboratory
Berkeley, California

AEC Contract No. W-7405-eng-48

MOLECULAR BEAM STUDIES OF SCANDIUM MONOFLUORIDE

David W. Green

(Ph.D. Thesis Part I)

January 1968

MOLECULAR BEAM STUDIES OF SCANDIUM MONOFLUORIDE

David W. Green

Inorganic Materials Research Division, Lawrence Radiation Laboratory,
Department of Chemistry, University of California,
Berkeley, California

ABSTRACT

The molecular beam method used previously to fix the electronic ground-state of lanthanum monoxide has been modified and extended to scandium monofluoride. King furnace equilibrium studies of the intensities of the green $^1\Pi$-$^1\Sigma^+$ and red $^3\phi$-$^3\Delta$ transitions have given the relative transition probabilities from both absorption and emission. From this data the expected relative intensity of the transitions in the molecular beam has been calculated assuming no radiative intersystem decay. The relative fluorescent intensity at various molecular beam path lengths indicates that both the $^1\Sigma^+$ and $^3\Delta$ states of ScF persist at least as long as 10^{-4} seconds. A maximum energy separation has been estimated to be 3,000 K (cm^{-1}).

The thermodynamic free-energy function is dependent upon the degeneracies and energies of these low-lying electronic states. This work indicates the partition function should include electronic, vibrational and rotational contributions from both the $^1\Sigma^+$ and $^3\Delta$ states. In addition, an unobserved $^1\Delta$ state should be thermodynamically important. Free-energy functions have been calculated using the best data available from this work.

It has been estimated that the $^1\Pi$-$^1\Delta$ transition has a small f-value and will be weak in emission compared to the $^1\Pi$-$^1\Sigma^+$. The ratio of the f_{abs} value of the $^3\phi$-$^3\Delta$ to that of the $^1\Pi$-$^1\Sigma^+$ is 0.8±3.

I. INTRODUCTION

A very successful model has been developed for atoms which predicts the lowest-energy electronic configuration. The lowest spectroscopic state arising from a given configuration may be obtained by applying Hund's rules. Furthermore, optical atomic spectroscopy has established not only the lowest energy level, but the energies of a multitude of excited states for many atoms. In some cases, energy levels of several positive ions have been determined from their spectra.

In striking contrast, few energy levels are known for most diatomic molecules. With the possible exceptions of N_2, CO and other ten valence electron molecules, most diatomic molecules have relatively low-lying energy levels which have not been spectroscopically observed. In many important molecules even the electronic ground-state is not known with certainty. This is especially true of species whose study is hindered by the relative difficulty of working at high-temperatures.

Diatomic oxides and halides of the transition metals are important high-temperature vapor species, yet only a few of the molecular states arising from ground-state atoms have been spectroscopically observed.

In addition, no universally applicable model or set of rules has been established for diatomic molecules. There are at least two useful models which predict approximate positions for molecular energy levels, but neither is presently capable of accurately resolving cases of nearly degenerate levels. This is especially true for the transition metal oxides and halides where the elements have a multitude of low-lying atomic and ionic states. The factors which lead to the stability of molecular states in these cases are not well-understood.

In high-temperature systems such as plasmas, jets or flames the chemistry is quite different from the more familiar room-temperature chemistry.[1] Unusual valence states have been observed. Diatomic molecules which are essentially non-existent at lower temperatures can become dominant vapor species at elevated temperatures. Containers and impurities become important parts of the systems. Oftentimes erroneous conclusions have been made from experimental data because of neglect of the effect of graphite or metallic containers upon the activity of the species under study. Vapor species resulting from impurities or the container can be a significant component of the total vapor in a high-temperature system.

Accurate thermodynamic data are lacking for many systems, in part due to the experimental difficulties of high-temperature studies. Free-energy functions obtained from statistical mechanical calculations are often more accurate than experimentally determined values. A third-law experimental approach normally makes use of a calculated partition function to obtain heats of formation. The free-energy function may be calculated from the partition function, Q, as follows for a diatomic molecule.

$$-\left(\frac{F^\circ - H_0^\circ}{T}\right) = R \ln Q \qquad (1)$$

The partition function can be approximated as the product of a translational part, a rotational part, a vibrational part and an electronic part. In this case the free-energy is the sum of separable contributions. The electronic partition function is written as follows:

$$Q_{el} = \sum_{\substack{\text{all} \\ \text{states}}} g_i \exp(-\epsilon_i/kT) \qquad (2)$$

$$= g_0 + g_1 \exp(-\epsilon_1/kT) + \ldots$$

In Eq. (2), g_i is the electronic degeneracy of the i^{th} electronic state and ϵ_i is its excitation energy. Normally only a small number of terms give appreciable contributions to the electronic partition function. In many molecules at low temperatures the only contribution is from the electronic ground-state. Since many common gases have $^1\Sigma$ ground-states whose degeneracy is one, there is no electronic contribution to the free-energy function. On the other hand, for high-temperature species, where there are often a number of states appreciably populated, this contribution to the free-energy function is very dependent upon the precise location of all the low-lying molecular states.

For example, for scandium monofluoride the lowest known triplet state is a $^3\Delta$ and the lowest known singlet is $^1\Sigma^+$.[2] If the singlet's contribution to the partition function were negligible because the triplet were considerably lower in energy, then there would be an electronic contribution of 3.58 calories $degree^{-1}$ $mole^{-1}$ to the free-energy function. On the other hand, if the triplet's contribution to the partition function were negligible, there would be no electronic contribution to the free-energy function. It should be added that there is an additional effect in the total free-energy function of ScF due to the unequal contributions of the singlet and triplet to the rotational and vibrational components. Since the vapor pressure of a species is dependent upon the exponential of free-energy, errors of this sort are most apparent in the vapor pressure. Calculated vapor pressures could be in error by a factor of ten or more due to the neglect of the contribution of one electronic state to the partition function.

Another example of a slightly different kind is magnesium oxide where the lowest observed state is assigned $^1\Sigma^+$.[3] Molecular orbital considera-

tions[1] predict a low-lying $^3\Pi$ and $^3\Sigma^+$ with degeneracies of six and three respectively. No triplet transitions have been observed. The large degeneracies of the triplets might be expected to dominate the partition function at high-temperatures if they are low-lying.

It is clear that accurate thermodynamic data for a diatomic molecule requires, most importantly, the electronic ground state and in many cases a precise knowledge of other low-lying electronic states.

Scandium monofluoride was chosen for study primarily for three reasons. Scandium is the lightest element with a d-electron in its ground-state atomic configuration. In aerospace applications and other high-temperature systems metals undergo chemical reactions with gaseous oxides, halides and nitrides. Diatomics and polyatomics are formed which involve bonding by d-electrons. The role of d-electrons is not well-understood and accurate predictions of the energies of low-lying electronic states is not possible. It seems incumbent to understand well the behavior of scandium in forming simple diatomics in order to allow some estimates to be made of the thermodynamic and bonding properties of all transition metal high-temperature species. Scandium fluoride is isoelectronic in valence electrons with titanium oxide. The TiO spectrum has been observed in M-type stars and is important for understanding some astrophysical processes. The ScF and TiO spectra are quite similar and analogies may be drawn between the two. A more complete knowledge of ScF should aid the interpretation of energy levels in TiO. Also a relatively low temperature is required for obtaining significant ScF vapor concentration. Many experimental errors increase rapidly as the temperature is increased so that low working temperatures are desirable.

II. PREVIOUS RESULTS

A. Methods of Determining Electronic Ground-States

The electronic ground-state of a diatomic molecule may be determined in several ways. The most direct method is the observation and analysis of a "forbidden" intercombination transition. This method is applicable to those molecules where sets of transitions of different multiplicity have been analysed. Such is the case in ScF where seven singlet electronic states and four triplet states have been identified.[2] The singlet energies are well-known relative to one another and the same is true for the triplets, but the energy of the group of singlets relative to the group of triplets has not been established.

The Vegard-Kaplan bands of N_2 and the Cameron bands of CO are examples of observed intercombinations in relatively light diatomic molecules. In heavier diatomic molecules where Hund's coupling case c is more closely approached, the selection rule $\Delta S = 0$ is not rigorous.[4] This means that the intercombination bands will have a larger transition probability. The strong visible bands of I_2 are, in Hund's coupling case a nomenclature, a $^3\Pi$-$^1\Sigma^+$ electronic transition which would be a forbidden transition if the coupling were pure Hund's case a. However in diatomic molecules of the first transition series, it is expected that most molecular states will be closer to Hund's cases a or b rather than case c. The selection rule of $\Delta S = 0$ has applicability and intercombinations may be considerably weaker in intensity.

In order to analyze a forbidden intercombination the transition must lie in a spectral region which is relatively free of allowed transitions. In the case of transition metal diatomic molecules which have so many allowed electronic transitions, this is extremely difficult since the greater ex-

posure times required would blacken the photographic plate with lines of allowed transitions.

Even though it does present experimental difficulties of some magnitude, analyses of intercombinations is an exact method. Not only can the electronic ground-state be determined, but the relative energies of all observed states will be known. The thermodynamic free-energy function is then subject only to errors caused by the neglect of unobserved states.

A second method which also has the advantage of determining relative energies as well as the identity of the ground-state is an analysis of rotational perturbations. This method is also applicable to diatomic molecules where sets of transitions of different multiplicity are observed.

When rotational energy levels of two electronic states have about the same energy at the same J values, they interact subject to certain symmetry and overlap restrictions.[4] This interaction is a mixing of the two energy levels such that each one takes on some of the characteristics of the other. These hybrid states repel one another resulting in the appearance of spectral rotational lines at energies other than what would be expected from the observation of lower and higher rotational levels. One of the selection rules is that the electronic states should have the same multiplicity. As in the case of intercombination bands, $\Delta S = 0$ breaks down as the mass of the diatomic molecule increases. It is these forbidden perturbations which yield information about the relative energies of states of different multiplicity. High resolution spectroscopic instruments allow measurement of the positions of rotational lines to within .02 K in most spectral regions. A Kaiser (K) is equivalent to wave numbers of cm^{-1}. Very small interactions can be detected by accurate measurement.

This method has been utilized successfully in the analysis of the spectrum of C_2[5,6] where shifts of equal magnitude and opposite direction were observed in the $A' \, ^3\Sigma_g^-$ and the $x \, ^1\Sigma_g^+$ states. In this relatively light molecule shifts of up to .32 K were observed so that in heavier molecules perturbations might be even more easily detected.

This method has the disadvantage that it requires accurate analysis of a number of bands in most cases. The lines exhibiting shifts from perturbations by other electronic states must be free from overlap of other lines of the same band, atomic lines, impurity lines or bands and lines from other bands of the same molecule. In addition, they must be in a vibrational band that can be analyzed. Despite these limitations, this method seems to be a potentially useful tool for molecules other than C_2.

A third method for determining the relative energy of two electronic states involves the variation of intensity with temperature. The intensity of a transition between two states, n and m, is given by a product,

$$I_{em}^{n,m} \propto \nu_{nm}^4 \; |R^{nm}|^2 \; \exp(-\nu_n \, hc/kT) \qquad (3)$$

where ν_{nm} is the frequency of the transition, R^{nm} is the matrix element of the transition and ν_n is the absolute excitation energy of the upper state, n.

This intensity may be compared to the intensity of another transition between states n' and m' where n' and m' are of different multiplicities than n and m. Let $R(T_1)$ and $R(T_2)$ be the ratios of intensity of the two transitions at two different temperatures.

$$K \equiv \frac{R(T_1)}{R(T_2)} = \frac{\exp[-\nu_n \, (1/T_1 - 1/T_2) \, hc/k]}{\exp[-\nu_{n'} \, (1/T_1 - 1/T_2) \, hc/k]} \qquad (4)$$

This comparison results in the cancellation of all terms except the Boltzmann excitation factors at the two temperatures. This equation may then be solved for $\Delta\nu$, the energy difference between the two upper emission states.

$$\Delta\nu = \frac{-T_1 T_2}{T_2 - T_1} \frac{k}{hc} \ln K \qquad (5)$$

This method has been applied to TiO[7] where the energy separation between the $^1\Delta$ and $^3\Delta$ has been determined.

Principal errors of this method are concerned with the measurement of accurate temperatures and intensities. A knowledge of the experimental conditions is required in order to interpret observations. Equation (3) assumes an equilibrium at temperature T which is never exactly true in a high temperature system. Line shapes and self-absorption corrections must be applied. There are also other temperature-dependent errors which can lead to erroneous interpretations of data.

A study of relative intensity vs temperature is, in principle, a good method for determining not only the electronic ground-state but the energy separation of states of different multiplicity. The experimental problems are great and accurate results are difficult to obtain. If the previously-mentioned methods cannot be applied, then this method serves as an indication of which states might be low-lying. In cases of large energy separation, this method may, despite its limitations, give the electronic ground-state and the energies of excited states accurately enough for the determination of the partition function at most temperatures.

Another method which has been applied to several diatomic molecules is matrix isolation. High-temperature species are "isolated" at low temperatures

by surrounding the molecules with "unreactive" atoms or molecules, usually a rare gas. In this manner the gaseous phase is simulated at liquid hydrogen (20°K) or liquid helium (4°K) temperatures. The Boltzmann excitation at these temperatures is small such that only low rotational levels of the first vibrational level of the lowest electronic state has any appreciable population. Light absorption by the isolated species should then correspond to gaseous phase absorption from the ground-state.

The disadvantage of this method is the interpretation of interactions between the isolated species and the host matrix. When comparing matrix isolated electronic transitions to the "same" transition in the gaseous phase, differences larger than 1000 K have been reported[8] in more than one case. Shifts between 200 and 1000 K are common. The interactions which are the origin of these shifts are not well-understood and predictions are subject to many exceptions. The interactions appear to be a complex sum of several factors including geometry, molecular size relationships, polarization effects, and energy transfer within the matrix system.

A particularly troublesome case is that of C_2 where the gaseous phase excitation of the $X^3\Pi_u$ is approximately 600 K. In matrix isolation studies, absorption transitions have been reported[8] involving both this state and the gaseous phase ground-state, $x^1\Sigma^+$. If experimental interpretations are valid, then this case is of particular interest. The satisfactory explanation of this phenomenon could allow predictions of the behavior of other high-temperature species in matrix isolation. At present, there is no adequate explanation. It seems that accidental degeneracy as an explanation can be eliminated because the transitions are observed in different host matrices where the interactions are considerably different. A separation in energy

between the two electronic states of more than 100 K in the matrix would probably eliminate any possibility of simultaneous Boltzmann excitation of the two electronic states.

Until more theoretical and experimental data are available, matrix isolation techniques have severe limitations for this kind of high-temperature problem. It is not clear, for example, what the relative interaction of two electronic states of different multiplicity might be. In cases of nearly degenerate electronic states, it is not clear whether the lower state in the gaseous phase always remains the lower state in matrix isolation. As with the method involving the temperature dependence of intensity, matrix isolation should determine the electronic gaseous-phase ground-state in cases of large energy separation.

It should be pointed out that no information is obtained from matrix isolation about the excitation energy of other low-lying states. In order to determine the partition function of a vapor species, it is necessary to know in some cases the excitation of low-lying states. If, for instance, the electronic ground state of ScF were $^1\Sigma^+$, the partition function could still be dominated by the $^3\Delta$ state because of its large degeneracy if the $^3\Delta$ were within a few thousand wave-numbers of the $^1\Sigma^+$ in the gaseous phase.

Matrix isolation is a potentially useful tool. It frees the spectrum of much complexity and overlap because of the small degree of thermal excitation. The method has been applied to several diatomic molecules in several host matrices and does appear to have wide applicability. It may well be possible to extend the scope of useful high-temperature information available from studies of this type when accurate interpretations become possible. However, until this happens, interpretations of gaseous phase

properties of diatomic molecules from the observed matrix isolation spectra should be done with regard for the limitations of the method.

Computers have made possible quantum mechanical calculations of molecular properties for a great many diatomics. In particular, the total energy of molecular states can be calculated by the self-consistent field methods of Roothaan[9] using linear combinations of atomic orbitals in a molecular orbital scheme. A full discussion of this field is beyond the scope of this paper.[10] An evaluation of the results of the work pertinent to scandium monofluoride is contained later in this paper. Suffice it to say that although great progress has been made in recent years, molecular calculations are not capable of accurately resolving relative energies in those cases where levels of different molecular orbital configurations are nearly degenerate. Correlation energies, which form a substantial portion of the total energy, are semi-empirical estimates of factors not accounted for in the molecular calculations and are subject to sizable errors in some cases. The quantities of interest are differences of large numbers causing the percentage uncertainty to be much greater in the difference than in the numbers themselves.

B. Summary of Previous Work on Scandium Monofluoride

Gaseous phase analysis of ScF has been done primarily by Barrow and associates.[2,11,12,13] Partial rotational analysis has been completed on transitions involving seven singlet and four triplet electronic states. Their experimental work was done in a carbon tube furnace at temperatures around 2000°C. The spectra were observed both in absorption and thermal emission. The lowest observed states of each multiplicity are $^1\Sigma^+$ and $^3\Delta$.

The energies of the singlets relative to one another and the triplets relative to one another has been well established.[2] Absorption was seen at 2000°C from both the lowest singlet and the lowest triplet. A diagram of the term energies obtained in their work is presented later in this paper.

Matrix isolation of ScF has been accomplished by McLeod and Weltner[14] using an inductively heated tungsten cell containing scandium metal and scandium trifluoride. They studied absorption from neon matrixes at 4°K and correlated their observations with the gaseous phase singlet transitions. Matrix shifts up to 500 K were observed although most were smaller. Extra features especially in the infrared were attributed to multiple sites in the matrix lattice and to other fluorides of scandium. Some features obtained in fluorescence in the matrix were not explained. It appears reasonable to conclude that the matrix isolated state of ScF corresponding to the gaseous phase $^1\Sigma^+$ state is the lowest electronic energy level in the neon matrix.

Calculations for ScF were done by Carlson and Moser[15] using the method of Roothaan. Their preliminary results gave a $^3\Delta$ electronic ground-state, but an extended basis set with corrections for correlation energy applied gave a $^1\Sigma^+$ ground-state. Calculations were simultaneously done for the isoelectronic TiO molecule and comparisons were made for the three lowest states. From the σ^2 molecular orbital configuration we get one state, $^1\Sigma^+$, while the low-lying $\sigma\delta$ configuration gives both $^3\Delta$ and $^1\Delta$ molecular electronic states. The values calculated by Carlson and Moser for the T_e values (term energy of the electronic state relative to the electronic ground-state) of these three states in both molecules is summarized in Table I in units of K.

Table I. Calculated[15] term energies for ScF and TiO in K.

Molecule	State	T_e(calc.)	T_e(calc. + corr.)	T_e(obs.)
	$^1\Delta$	176	2610	
ScF	$^3\Delta$	-4540	460	
	$^1\Sigma^+$	0	0	0
	$^1\Delta$	4430	2150	580
TiO	$^3\Delta$	0	0	0
	$^1\Sigma^+$	13240	6690	2290

The $^1\Sigma^+$ is chosen as the zero of energy in ScF while it is the $^3\Delta$ in TiO. The first column is the term energy calculated using their extended basis set. The second column is a corrected term energy which neglects core polarization and relativistic effects but includes configuration interaction estimates obtained by a consideration of the atomic orbitals involved. The third column contains the observed values where they are known. The $^1\Sigma^+$ state of ScF is taken to have a zero observed energy on the basis of the matrix observations. The observed values for TiO are based on the work of Phillips.

It should be noted that there is an error of about 4400 K in the calculated separation of the $^1\Sigma^+$ and $^3\Delta$ in TiO assuming the experimental values to be correct. If the same magnitude of error applies to ScF, then the ground-state could well be either $^3\Delta$ or $^1\Sigma^+$. If the errors are larger in ScF than in TiO, the electronic partition function at most temperatures is uncertain. Its error could easily be a factor of six based on these calculations.

III. THEORY

A. Predictions for ScF

Scandium fluoride, titanium oxide and zirconium oxide are isoelectronic in valence electrons and it would be expected on the basis of molecular orbital considerations that their electronic spectra should show similarities. The electronic spectrum of TiO has been known for some time and its spectrum has been well studied.[7,16-33] ZrO is less studied, but its spectrum is also reasonably well-known.[24,31,34-38] The correspondence of the electronic states of these three molecules is shown in Fig. 1. The data are assembled from previously mentioned references. Data are not available for all the energy separations so some estimates were made. For TiO the $^3\Delta$-$^1\Delta$ separation was taken from the work of Phillips. For ZrO neither the $^1\Sigma^+$-$^1\Delta$ separation nor the $^1\Sigma^+$-$^3\Delta$ separation is known. The $^1\Sigma^+$ state has been seen in matrix isolation[38] so it was chosen as the ground-state. It is expected from Hund's rules that the $^3\Delta$ is lower in energy than the $^1\Delta$ since both states arise from the same molecular orbital configuration. This separation was taken to be the same as in TiO and the $^3\Delta$ was arbitrarily put at 1000 K. For ScF the $^1\Sigma^+$ and $^3\Delta$ were both put at the zero of energy. The $^1\Delta$ has not been observed in this molecule and was put at 2000 K.

The similarities are noticeable from this energy level diagram. The three low-lying states are probably nearly degenerate in all three molecules. The second excited observed singlet state is a $^1\Pi$ for all molecules if we assume that the unobserved $^1\Delta$ state is below about 5000 K in ScF. The first observed excited triplet is a $^3\phi$ and a $^3\Pi$ lies slightly above in all three molecules.

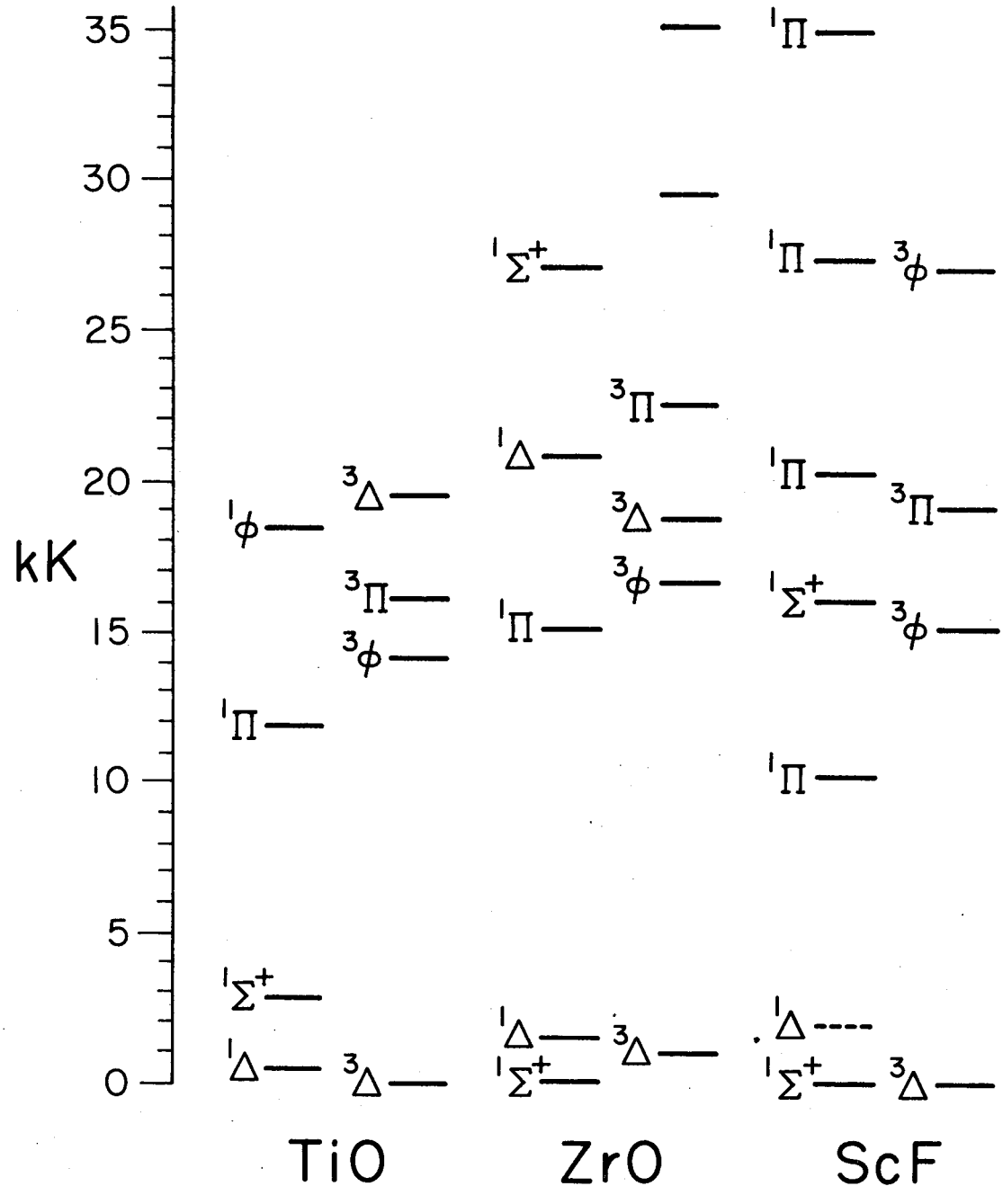

XBL6711-5676

Fig. 1 Electronic energy levels of isoelectronic TiO, ZrO and ScF.

Using the TiO and ZrO energy levels, we might predict for ScF the near degeneracy of the $^3\Delta$ and $^1\Sigma^+$. There should also be a low-lying $^1\Delta$ state possibly within 2000 K of the ground-state. Perhaps there is a $^3\Delta$ excited state near 20,000 K. Care should be taken in empirical correlations of this sort. It is by no means clear from these considerations what might be the electronic ground-state. This correlation does appear to be useful as a starting point for suggesting useful experimental methods to resolve some of the energy difference questions.

It is useful in many molecules to consider what molecular states arise from the combination of low-lying atomic states. The electronic ground-state of fluorine is $^2P^\circ$ from the $1s^2 2s^2 2p^5$ configuration. The first excited state is over one hundred thousand wave numbers higher in energy[39] and need not be considered. The ground-state of scandium is ^2D from the $4s^2 3d$ open-shell configuration. Furthermore scandium has low-lying electronic levels from the $4s3d4p$ and $4s3d^2$ configurations which may well combine with the $^2P^\circ$ state of F to give low-lying molecular states. Figure 2 shows those states of scandium below 30,000 K. Table II lists the states which arise from the combination of ground-state F with the low-lying states of Sc.[4]

There are eighteen molecular states arising from ground-state atoms alone. It is difficult to predict a priori which of these states might be stable. There are, furthermore, a multitude of electronic molecular states arising from low-lying excited atomic states. In addition, the three molecular states arising from $Sc^+(^3D) + F^-(^1S)$ should be considered. In a diatomic molecule formed from atoms of such different electronegativity, these ionic states could be quite low in energy.

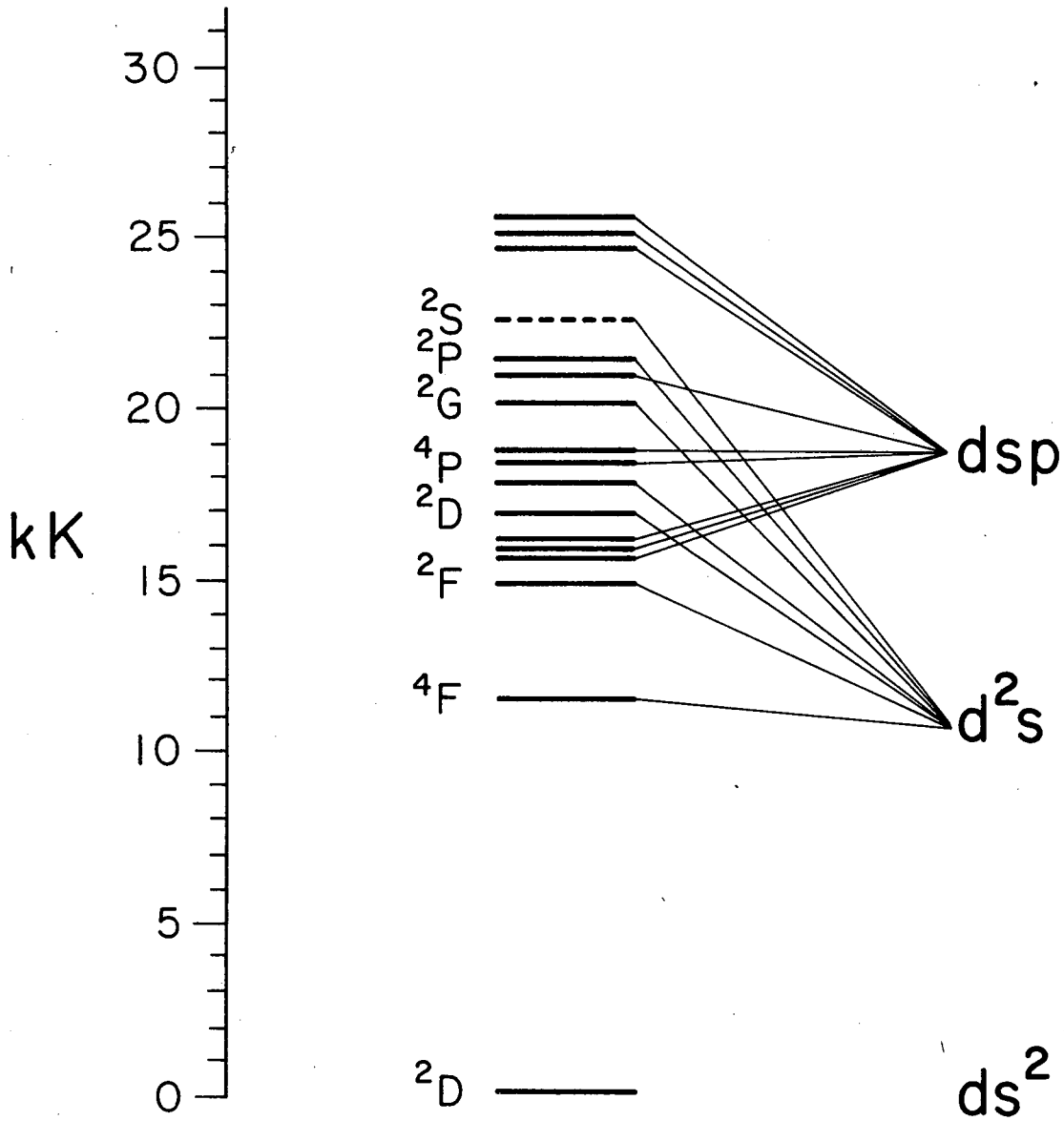

Fig. 2 Electronic energy levels of scandium atom.

Table II. Molecular states of ScF from atomic configurations.

Sc State	F State	Molecular states of ScF	Multiplicities
^2D	$^2P^o$	$\Sigma^+(2)$, Σ^-, $\Pi(3)$, $\Delta(2)$,ϕ	1,3
^4F	$^2P^o$	Σ^+, $\Sigma^-(2)$, $\Pi(3)$, $\Delta(3)$,$\phi(2)$, Γ	3,5
^2F	$^2P^o$	Σ^+, $\Sigma^-(2)$, $\Pi(3)$, $\Delta(3)$,$\phi(2)$, Γ	1,3
$^4F^o$	$^2P^o$	$\Sigma^+(2)$, Σ^-, $\Pi(3)$, $\Delta(3)$,$\phi(2)$, Γ	3,5
$^4D^o$	$^2P^o$	Σ^+, $\Sigma^-(2)$, $\Pi(3)$, $\Delta(2)$,ϕ	3,5

It should be evident that this approach gives little useful information about which molecular states are low-lying or which state might be the ground-state. In general, this is not true, but for transition metal diatomics this is often the case. The d-electrons give rise to atomic states of high angular momentum. Coupling of these momenta to those of the P states of oxygen or a halogen gives a large number of molecular states. The proximity of the s, p and d orbitals complicates this approach since low-lying molecular states may dissociate to excited atoms. And finally, the molecular states arising from ionic configurations cannot be neglected.

These considerations demonstrate well that the spectra of diatomic molecules formed from transition metals can be expected to be complicated. There will be numerous allowed transitions. In addition it is expected that interactions causing perturbation and predissociation will be common.

A different approach is to consider the molecular orbitals involved. Neglecting the inner filled main shells of scandium and fluorine, the orbitals of importance should be the $2p\sigma$ and $2p\pi$ from fluorine and the $4s\sigma$, $4p\pi$, $4p\sigma$, $3d\sigma$, $3d\delta$ and $3d\pi$ of scandium. It has been shown[15] that this

population analysis is a good approximation to the molecular orbitals of ScF. Table III suggests molecular orbital configurations for the observed states of ScF. All states observed, with the exception of the highest energy $^1\Delta$, can be accounted for by considering the Sc $3d\sigma$, $3d\pi$, $3d\delta$, $4p\sigma$ and $4p\pi$ orbitals as low-lying. The lowest three states come from the nearly degenerate $3d\sigma$ and $3d\delta$ orbitals. All excited states are various combinations of other low-lying orbitals with these two.

This method is a useful approach to ScF in some respects. As applied here it is used after states have been observed. It might equally well have been used to predict the ScF energy levels by looking at the observed TiO states to determine the relevant orbitals. Then using the results of calculations to predict trends, the states of ScF could have been estimated. However, the approach is also limited in accuracy and it is of questionable use in predicting the electronic ground-state ScF.

There are two electronic states predicted by this consideration which could well be important to the thermodynamic properties of ScF. The unobserved $^1\Delta$ should be within 5000 K of the ground-state and perhaps even lower. A $^3\Pi$ state which is unobserved in TiO, ScF, and ZrO should, by Hund's rules, be lower than the $^1\Pi$ state at 10,600 K in ScF. The prediction of these unobserved states makes this approach of great value. As a larger number of electronic states become known, the energies of the unobserved states can be predicted with a reasonably high degree of accuracy.

B. Outline of Experimental Approach

In low resolution the triplet band system of ScF which is most characteristic is the $A^3\phi$-$X^3\Delta$ with (0,0) heads at 6523, 6540 and 6558 Å.[13] It is red degraded and free of significant overlap from other bands of the same electronic transition as well as bands of other electronic transitions. The

Table III. Molecular states of ScF from molecular orbitals.

Molecular Orbital Configuration	Molecular State	Approx. Observed Energy (kK)
$p\sigma^2\ s\sigma^2\ p\pi^4\ d\delta\ d\sigma$	$^3\Delta$	0.0
	$^1\Delta$	
$d\sigma^2$	$^1\Sigma^+$	0.0
$d\sigma\ d\pi$	$^3\Pi$	
	$^1\Pi$	10.6
$d\delta\ d\pi$	$^3\phi$	15.3
	$^3\Pi$	18.3
	$^1\phi$	
	$^1\Pi$	20.3
$d\sigma\ p\sigma$	$^3\Sigma^+$	
	$^1\Sigma^+$	16.1
$d\sigma\ p\pi$	$^3\Pi$	
	$^1\Pi$	26.8
$d\delta\ p\pi$	$^3\phi$	27.2
	$^3\Pi$	
	$^1\phi$	
	$^1\Pi$	34.9

(0,1) head of the $E^1\Pi$-$X^1\Sigma^+$ transition at 5115 Å is also strong in low resolution. These two transitions involve the lowest states of each multiplicity, namely the $^1\Sigma^+$ and the $^3\Delta$. The relative intensity of these two transitions depends upon the population of the states involved, the oscillator strength or f-value of the transition and the method of excitation.

The strengths of these transitions were compared in a King furnace which is a good approximation to thermal equilibrium. They were again compared in a molecular beam coming from a cell of the same temperature after a transit time of approximately 10^{-4} seconds. Should intersystem radiative

decay occur within this time, the effect would be noticeable as an apparent decrease in intensity of either the singlet or triplet band system. In this manner the electronic ground-state can be determined experimentally while avoiding many of the temperature dependent errors of other methods.

In Hund's coupling case c the $^3\Delta_1$ to $^1\Sigma_0^+$ is an allowed transition. ScF is a reasonably heavy diatomic molecule and should have a large enough degree of case c coupling to make this transition possible. The lifetime of the $^1\Sigma^+$ (or $^3\Delta$) is dependent on the degree of case c coupling and the energy separation of the two states. Rough estimates indicate the lifetime could be either longer or shorter than the beam transit time of 10^{-4} seconds.

C. Relationship of Absorption, Emission and Fluorescence

Define an intensity ratio, R, as follows:

$$R = \frac{I(\text{triplet})}{I(\text{singlet})} . \qquad (6)$$

R is the ratio of intensities of any source at two particular wavelengths, namely, the 6558 Å ScF $^3\phi$-$^3\Delta$ (0,0) band head and the ScF $^1\Pi$-$^1\Sigma^+$ (0,1) band head (~5115 Å). All intensities are given in terms of number of quanta per second per square centimeter normal to the source per unit solid angle per unit wavelength interval.

In a high-temperature equilibrium source such as the King furnace, the intensity observed at a particular wavelength after passing light from a lamp at a temperature T_ℓ through a column of gas at a temperature T_g is given by:

$$I_{observed} = I_{lamp,T_\ell} - I_{abs}^{lamp} + I_{em} - I_{abs}^{self} . \qquad (7)$$

I_{abs}^{lamp} is the intensity of light coming from the lamp that is absorbed by the gas. I_{em} is the intensity of emission of the gas and I_{abs}^{self} is the absorption by the gas of the emitted light. The self-absorption will be small for small gas densities or path lengths and will be neglected here. Arguments will be presented later to justify this approximation.

An alternative expression is in terms of the observable apparent or net absorption.

$$I_{abs}^{net} = I_{lamp,\ T_\ell} - I_{observed}$$

$$= I_{abs}^{lamp} - I_{em} \qquad (8)$$

When a lamp with a brightness temperature equal to the gas temperature is used in the King furnace

$$I(\text{singlet})_{em,KF,T_g} = I(\text{singlet})_{abs,KF,T_g} \quad \text{and}$$

$$I(\text{triplet})_{em,KF,T_g} = I(\text{triplet})_{abs,KF,T_g} \quad \text{or}$$

$$R_{em,KF,T_g} = R_{abs,KF,T_g} = T_\ell \,. \qquad (9)$$

This is a statement of the reversal condition. I_{abs}^{net} becomes zero in Eq. (8) or $I_{observed}$ is equal to $I_{lamp,T_g = T_\ell}$ in Eq. (7).

At each wavelength, α is the absorption coefficient.

$$\alpha = \frac{I_{abs}^{lamp}}{I_{lamp,T_\ell}} \qquad (10)$$

Now α is directly observable only when I_{em} is negligible compared to I_{abs}^{lamp} or from Eq. (8) when $I_{abs}^{net} \sim I_{abs}^{lamp}$.

If a blackbody at the gas temperature were used as a lamp, then from the reversal conditions for either wavelength:

$$\alpha = \frac{I_{em,KF,T_g}}{I_{BB,T_g}} \tag{11}$$

The relationship between King furnace absorption and emission is now established. Experimentally a lamp at T_ℓ is used instead of a blackbody at the gas temperature, but the relationship of lamp intensity at T_ℓ to blackbody intensity at T_g is easily calculated from the Planck equation and the emissivity of the lamp filament. Then at each wavelength the following two equivalent relationships may be used to determine the absorption coefficient.

$$\alpha = \frac{I^{lamp}_{abs,KF,T_g}}{I_{lamp,T_\ell}} = \frac{I_{em,KF,T_g}}{I_{lamp,T_\ell}} \frac{I_{lamp,T_\ell}}{I_{BB,T_g}} \tag{12}$$

The ratio of emission intensities is now given from Eq. (11) by:

$$R_{em,KF,T_g} = \frac{\alpha(t)\ I(t)_{BB,T_g}}{\alpha(s)\ I(s)_{BB,T_g}}$$

$$= R_\alpha R_{BB,T_g} \tag{13}$$

The letters s and t represent the two wavelengths of interest (6558 and 5115 Å). By a similar consideration of Eq. (12), the ratio of α values may be obtained from King furnace absorption studies.

$$R_\alpha = \frac{R_{em,KF,T_g}}{R_{BB,T_g}} = \frac{R^{lamp}_{abs,KF,T_g}}{R_{lamp,T_\ell}} \tag{14}$$

It should be noted here that in the ratio of α's the dependence of α upon the absorption path length and gas density will divide out if the same system and geometry are used for both the singlet and triplet intensities. Thus, the α ratio depends only upon the relative triplet and singlet transition probabilities.

In the molecular beam, fluorescence is observed at right angles to an exciting light source. If we assume no significant population change of the lowest singlet and the lowest triplet during the beam transit time, then the equilibrium relative intensity measurements of the King furnace may be applied to determine the expected relative intensity in the beam. The fluorescent intensity observed depends upon the transition probability to the upper state of each system and the intensity of the exciting light at that wavelength. In addition there is a geometric factor which includes the differences between the geometry of the beam and that of the King furnace as well as the fact that fluroescence takes place in all directions. This geometric factor is the same for singlet and triplet so it will divide out in the intensity ratios. The ratio of fluorescent intensity in the beam is given by:

$$R_{f,B,T_g} = \frac{\alpha(t)\ I(t)_{ex}}{\alpha(s)\ I(s)_{ex}}$$

$$= R_\alpha\, R_{ex} \qquad (15)$$

R_{ex} is the ratio of exciting light intensities at the triplet and singlet wavelengths.

An implicit assumption in this formulation is that fluorescence occurs at the same wavelength as the absorption of light. In addition it is assumed that there are no additional methods of populating the upper fluorescent state. A correction factor must be applied to account for these two factors. This correction factor involves the Franck-Condon factors within the states under consideration and the loss of light due to other electronic transitions. A consideration of the internuclear distances of the four states involved in these two transitions suggests the corrections due to Franck-Condon factors will tend to cancel in part. The transition from the $^1\Pi$ state to the unobserved $^1\Delta$ may be of sufficient intensity to change the expected relative intensity. This correction factor may be distinguished from intensity change due to intercombination radiative decay by studying relative intensity as a function of the molecular beam path length. Whereas radiative decay is a function of the beam transit time, this correction factor is the sum of factors which are only functions of the molecule's relative transition probabilities. Except under unusual circumstances, this correction factor will not be a function of the beam transit time. Therefore this correction factor will only be considered in the final application of these equations.

Since, for reasons given later in this paper, the triplet transition is more easily seen, the most useful working equation is the prediction of the singlet intensity from the observed triplet intensity.

$$I(\text{singlet})_{f,B,T_g} = I(\text{triplet})_{f,B,T_g} \frac{1}{R_\alpha R_{ex}} \qquad (16)$$

So the expected singlet intensity in the molecular beam may be calculated from the experimental quantities: 1) the beam triplet intensity; 2) King furnace emission or absorption α value ratios; and 3) the beam exciting light intensity ratio.

D. Intensity Measurement and Photographic Equipment

Photoelectric equipment was not used in this work because of the extremely low light level in the molecular beam and because simultaneous measurement had to be made of four light levels. A photographic plate can integrate intensities over long periods of time and they are superior for the detection of weak sources at two wavelengths simultaneously. Interpretation of results requires a knowledge of that part of the intensity due to background.

The subject of photographic response is a complex subject and is not completely understood. The relationship between the density of silver obtained on a plate from the reduction of silver halide and the intensity of light causing the response may be studied in general terms. Experimental data are available on deviations from general response in particular exposure conditions.

The amount of light incident upon a photographic plate may be controlled by either changing the number of photons reaching it within a given time or by changing the time of exposure. A quantity E is defined to measure the amount of light and is called the exposure. It is defined as the product of the light intensity and exposure time and it gives the total number of photons incident upon the plate. The optical density, D, may be measured on the plate for a series of different exposures. The resulting plot of

optical density against log E is called an "H and D" curve or a "characteristic" curve.

Figure 3 shows an example of a characteristic curve which was obtained for 103 a-F photographic plates at 6558 Å. This curve was plotted on a log I scale since all the data points were obtained with equal exposure times. The units of log I are arbitrary. The relative scale is accurate and, for example, the density can be predicted for an intensity I' from a knowledge of the density produced by an intensity I if the ratio of I and I' is known.

Density is measured by directing a light beam through the photographic plate and measuring the intensity I. If I_0 represents the observed intensity with no photographic plate, then the density is the log of the ratio.

$$D = \log I_0/I \tag{17}$$

Figure 3 shows a linear region of response from a density of .4 to at least 2.0 which is the limit of measurement with the equipment used in this work. If log i represents the hypothetical intercept of this line with the log I axis, then the relationship between density and intensity may be expressed in mathematical form.

$$D = \gamma (\log E - \log i) \tag{18}$$

Generally, useful information can be obtained about the exposure only near the linear region of the characteristic curve. In this region experimental errors are minimized since a given exposure difference results in the largest optical density difference on the plate.

Plates are made from glass coated with an emulsion which contains a dye and a photosensitive material. Different emulsions give access to different

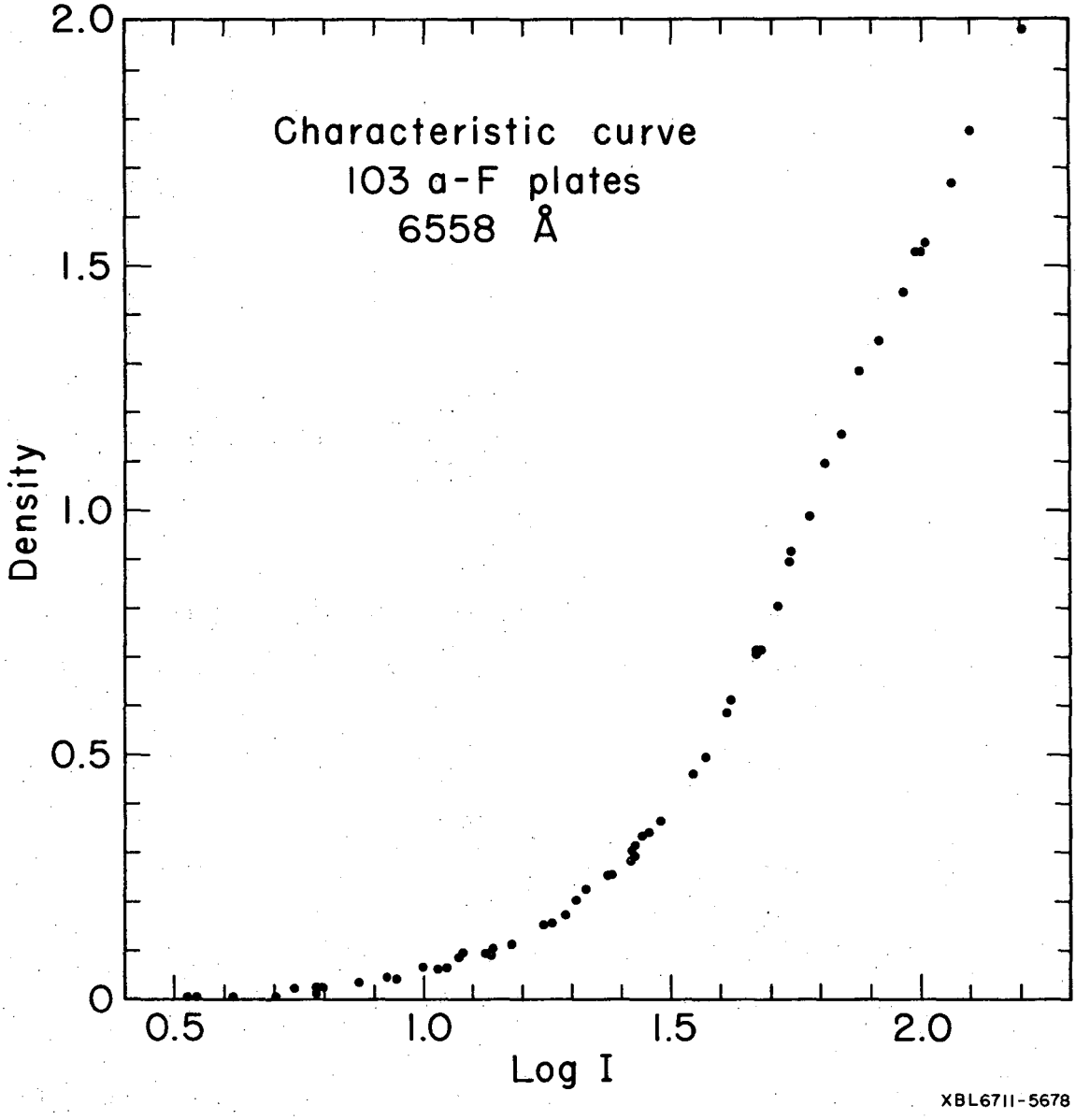

Fig. 3 Characteristic curve for 103 a-F photographic plates at 6558 Å.

spectral regions. Variation of silver halide grain size within the emulsion is used to get different sensitivity within a spectral region. The characteristic curve is dependent on both these factors as well as on the wavelength of the light.

Plates manufactured at different times have slight variations in their emulsions and consequently slight variations in their characteristic curves. Even within the same plate the emulsion is not completely uniform, but this is not generally an important source of error.

It has been experimentally demonstrated that γ is a strong function of both the time of development and the temperature of the developing solution.[40,41] For this reason γ is often referred to as the development factor. It is also a function of wavelength.

There are several deviations from the general conditions discussed above even if the shape of the characteristic curve is well controlled. One of the more important is called the "reciprocity effect."[40,41] A given exposure, E, does not result in the same optical density if the intensity and the exposure time are varied over large ranges. This effect becomes appreciable at very high or very low intensity levels where the plates show an apparent loss of sensitivity. For photometric work this plate characteristic requires identical exposure times for comparison of intensities. It has been shown[40] that for a constant plate density, It^p is constant where p is a constant of the order of 0.8. This is not valid over a large range, but is relatively good for a time interval of several minutes to a few hours. In this work the effect should not be appreciable, but can be entirely eliminated by using a constant exposure time while varying the intensity. Since only relative intensities are measured in this work, only the relative reciprocity effect is of any importance and this should be small.

In the measurement of optical densities from a plate, the Eberhard effect must be considered. The chemical and physical processes occuring at the boundary between a light and dark area of the plate cause anomalous effects. If an intensity step function of height from zero to a finite value A is used, the measurement of plate optical density will fall below zero as the step function is approached. It will rapidly rise above the density corresponding to A as the step function is entered and then fall to A giving a true reading. This effect is attributed to migration of developer solution from the low density region to the high density region.[40,41] The developer is exhausted in the high density region and the migrating fresh developer results in overdevelopment there at the expense of the low density development. This means sharp lines could give inaccurate characteristic curves while a continuum source at the same wavelength and intensity should be better.

A method of pre-exposure was used on most photographic plates in this work. A tungsten filament bulb, run from a variable transformer and a timer, was used as the light source. The entire plate was exposed to a level of light such that it was brought close to the linear region of the characteristic curve. In this manner, optimum use was made of any additional light falling on the plate. Weak features could be seen better since the region of maximum photographic response was used. The gross fog of the plate is increased, but since interest in this work is in the accentuated weak features, this loss of contrast was unimportant.

In some exposures a longer development time was used. This procedure also results in an increase of gross fog. There is an increase of γ which is useful for detecting weak features.

Because of the difficulties in accurately relating the optical density of a photographic plate to the intensity of light causing the photographic response, one should in principle calibrate each plate used at every wavelength used. In practice, it is found that the shape of the characteristic curve varies slowly as a function of wavelength and that the plate sensitivity for small wavelength intervals in the wavelength regions of interest is nearly constant. Furthermore, photographic plates produced at the same time have negligible variations in photographic response when used in an identical manner. This means that a characteristic curve should be experimentally found for each wavelength region of interest and this curve can then be used as a basis for comparison for other plates at the same wavelength. Extreme care must be taken to insure duplication of development conditions or the apparent photographic response will show significant variation.

IV. EXPERIMENTAL

A. Spectrographs

Two spectrographs were used in this work. A 0.75 meter Spex was used only for identification of spectra obtained from King furnace emission. The Spex has a Czerny-Turner kinematic mount for interchangable gratings. A reciprocal linear dispersion of about 10 Å/mm was obtained in first order using a 5000 Å blaze grating with 1200 lines per millimeter. Its aperture is f/6.8. This instrument is readily converted to use with several photographic and photoelectric detectors. Polaroid type 413 infrared film rolls were used in the red spectral region. Polaroid type 57 four inch by five inch film packets which have a speed of 3000 (ASA equivalent) were used for detection in the green spectral region. Polaroid type 55 four inch by five inch film packets give a negative as well as a positive which facilitates measuring of spectral features. Both types of polaroid packets have a panchromatic type B spectral response. Polaroid film and packets were used for preliminary work. More permanent exposures were recorded on Kodak 103 a-F photographic plates whose spectral response is nearly uniform throughout the visible region.

Quantitative results were obtained using a Steinheil three-prism instrument. Several interchangable configurations of prisms and lenses are available with the Steinheil and this work made use of a Raman arrangement. Its aperture is f/4. The collimator focal length is 195 millimeters and the camera focal length is 255 millimeters. The reciprocal linear dispersion varied with wavelength from about 30 Å/mm at 5000 Å to about 110 Å/mm at 6700 Å. The entire visible spectrum appears on the photographic plate in about six centimeters. The focus of the instrument is noticeably curved

in this optically fast arrangement. Simultaneous focus was obtained in the two spectral regions of interest using the cadmium red and green lines. The resulting prism positions and other instrumental adjustments were kept identical throughout the course of this study. Kodak 103 a-F photographic plates were used for detection. A slit size of .010 millimeters was used in all exposures to insure duplication of the appearance of spectral features.

B. King Furnace

A full description of the King furnace appears elsewhere.[42-44] Figure 4 is a photograph of the external features of the furnace.

Figure 5 shows a schematic diagram of the electrical connections. In typical operation there was a potential drop of nine to ten volts along the graphite resistance heating tube resulting in a current of approximately 1400 amperes. A 100 KVA step-down transformer with multiple connections provided temperature range selection. Fine temperature adjustment was obtained with a buck-boost variable transformer whose secondary was in series with the step-down transformer.

Graphite tubes with a bore of 1.25 cm were approximately 31.3 cm in length with a hot-zone of 15.0 cm. A taper on the tubes in the hot-zone minimized thermal gradients. It was observed that temperature variations at 2100°C were normally less than 20° throughout the hot-zone. The tubes were lined with .0025 cm thick tungsten foil next to the graphite to minimize the effect of reaction of scandium with graphite. Inside the tungsten, .0025 cm thick tantalum foil was used to simulate the container described later which was used in the molecular beam studies. At the ends of the hot-zone, graphite radiation shields with a bore of .63 cm were used to achieve a sharp temperature gradient to the water-cooled electrodes.

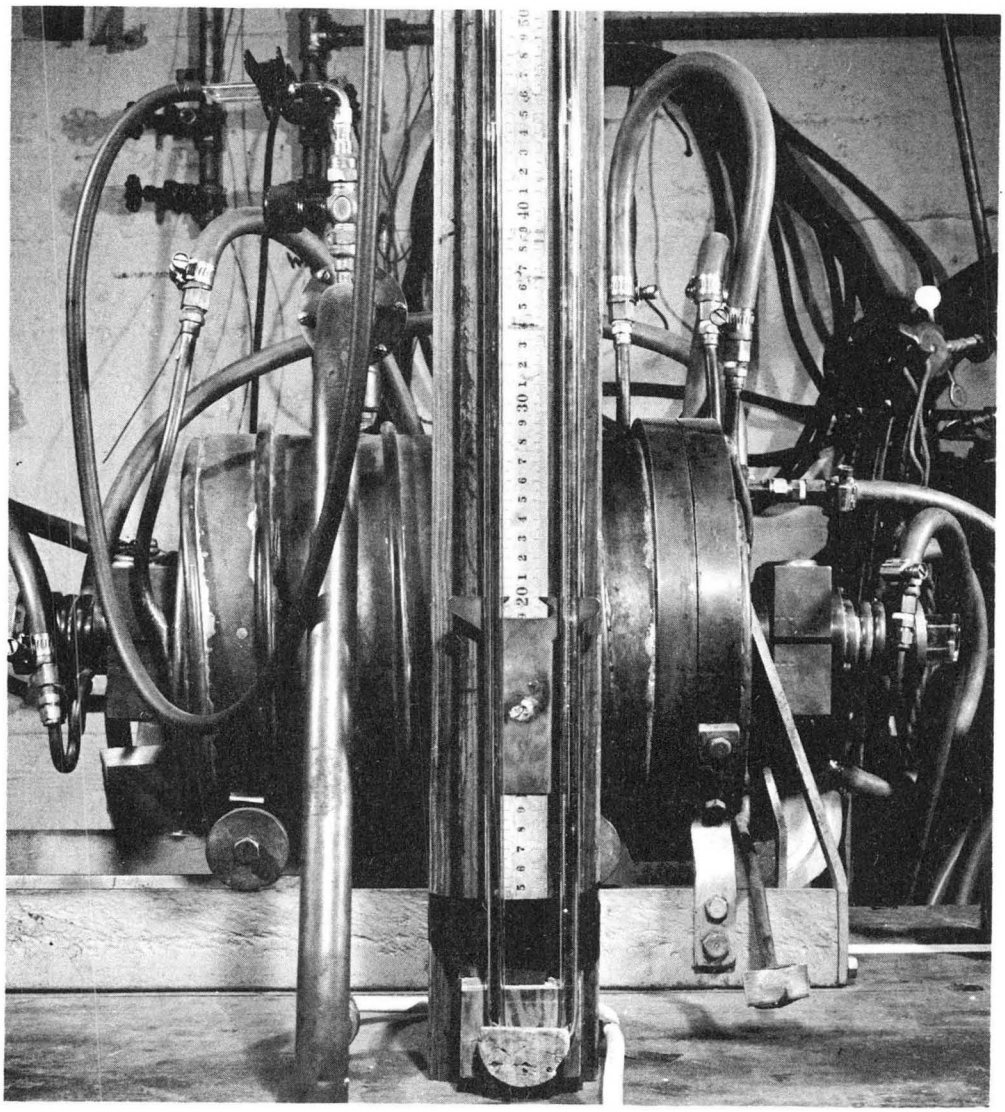

XBB 672-580

Fig. 4 External view of the King furnace.

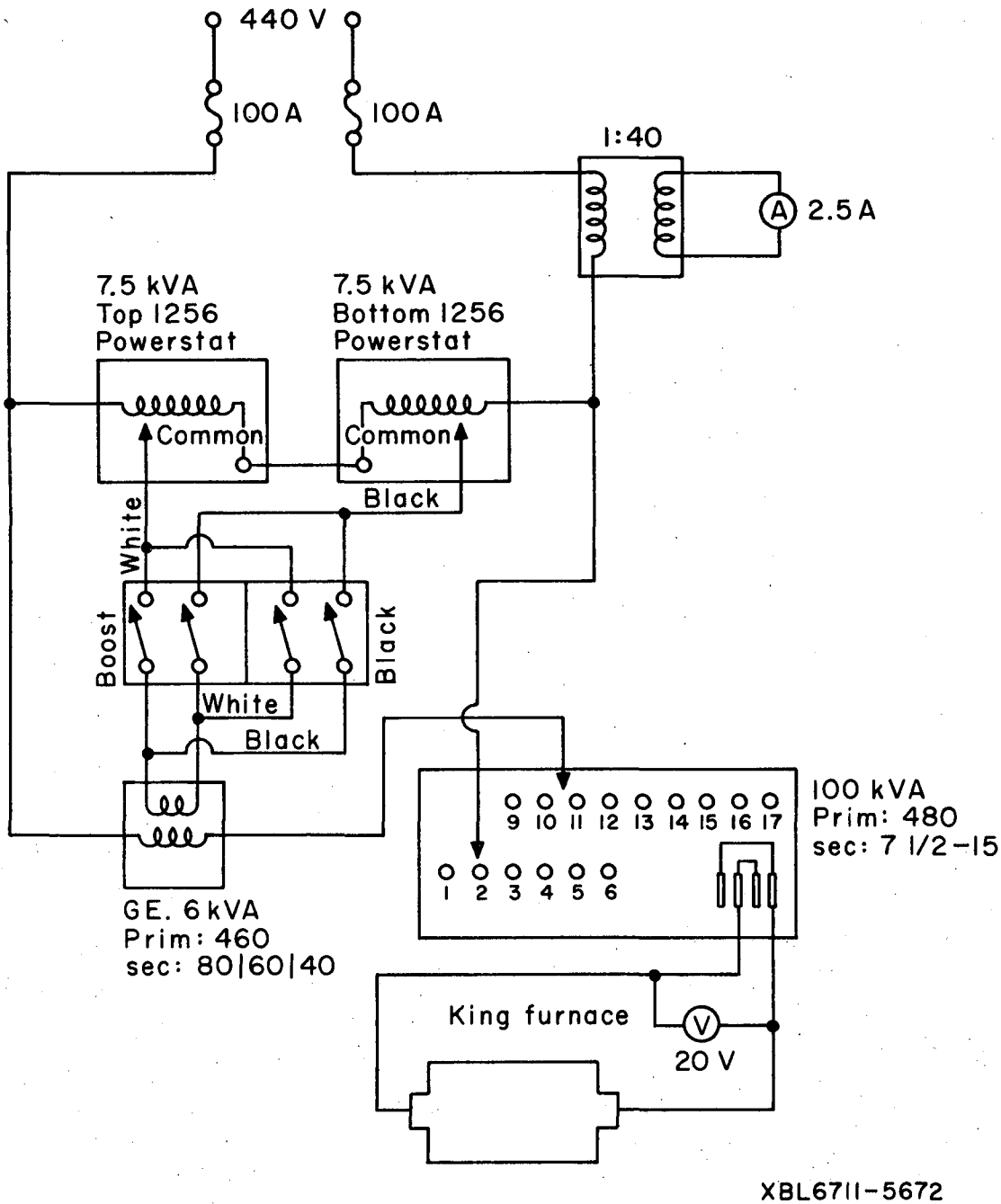

Fig. 5 Wiring diagram of the power supply for the King furnace.

Rare gas was added to the King furnace to hinder material loss to the cold regions of the furnace, aid temperature equilibration in the hot-zone, and, primarily, to prevent the acceleration of electrons. At the operating temperatures used, concentrations of free electrons are such that appreciable excitation of the species under study could take place. A potential difference of ten volts is sufficient to accelerate electrons to high energies relative to molecular energy levels. A pressure of sixty to one hundred torr of argon at room temperature prevented non-thermal molecular excitation at high-temperature.

Temperature measurements were made with a Leeds and Northrop optical pyrometer, catalogue number 8622-C-S. Corrections were applied for windows on the King furnace. The pyrometer was calibrated against a pyrometer with known scale corrections in order to obtain the true temperature from the scale readings. Reproducibility of measurements was better than five degrees. Calibration uncertainties are also the order of five degrees and since this pyrometer was not calibrated from a primary standard the uncertainty is probably ten degrees at the temperatures used. The manufacturer's specified accuracy is about twenty degrees at these temperatures. It has been shown[45] that the temperature measured from the King furnace walls approximate well the temperature of a blackbody. Therefore the emissivity of the King furnace walls is nearly one and no corrections were applied for this effect.

Absorption experiments were done with the optical arrangement of Fig. 6 where all measurements are in centimeters. The lamp filament was focused into the center of the furnace with a 16.7 cm focal length lens. After passing through the furnace the image was again focused by a 22.0 cm focal

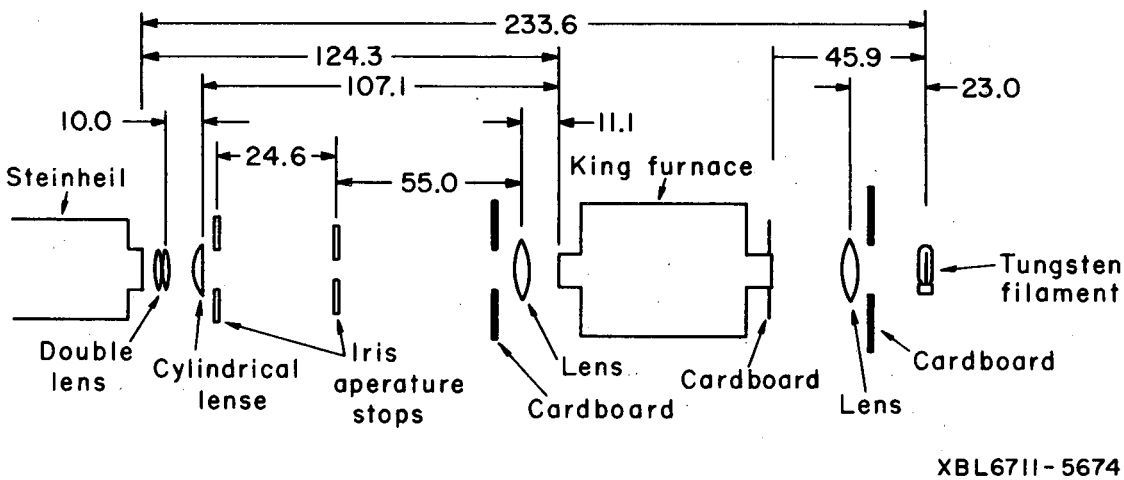

Fig. 6 Optical system for King furnace absorption.

length lens onto an iris diaphragm. A cylindrical lens focused one plane of the light onto the Steinheil slit while a double lens system with a combined focal length of 6.5 centimeters filled the collimator lens inside the Steinheil. A He/Ne laser was used to assure accurate alignment of all optical components on the optical axis. Visible checks of the focus of the lenses could be made prior to heating the King furnace.

Blackbody wall radiation, which could be minimized for accurate photometric studies, is of importance in the King furnace. Direct radiation from walls as well as light scattered from particles and dust within the hot-zone must be considered. The optical system of Fig. 6 shows several photographic cardboard light stops which were used to prevent stray light from entering the optical path. A variable iris diaphragm with a minimum opening of .5 mm was placed at the focal point of the image of the center of the furnace so that most of the wall radiation can be eliminated.

Figure 7 shows the schematic wiring diagram for the absorption lamp. A General Electric SR-8 tungsten strip filament which has adequate light at both wavelengths was used. It also has the advantage of having a filament whose emissivity has been studied so that the spectrum can be calculated for the quantitative work. The lamp was operated well over its rated six volts and eighteen amps. A wattmeter was used to control lamp conditions since it was felt that the temperature could be more accurately reproduced in different experiments by duplication of power input. Any deterioration of the lamp filament which results in a small resistance change would result in different power levels if either the current or voltage were kept constant. Line voltage fluctuations were eliminated with a constant voltage transformer. A power level of 215 watts was chosen

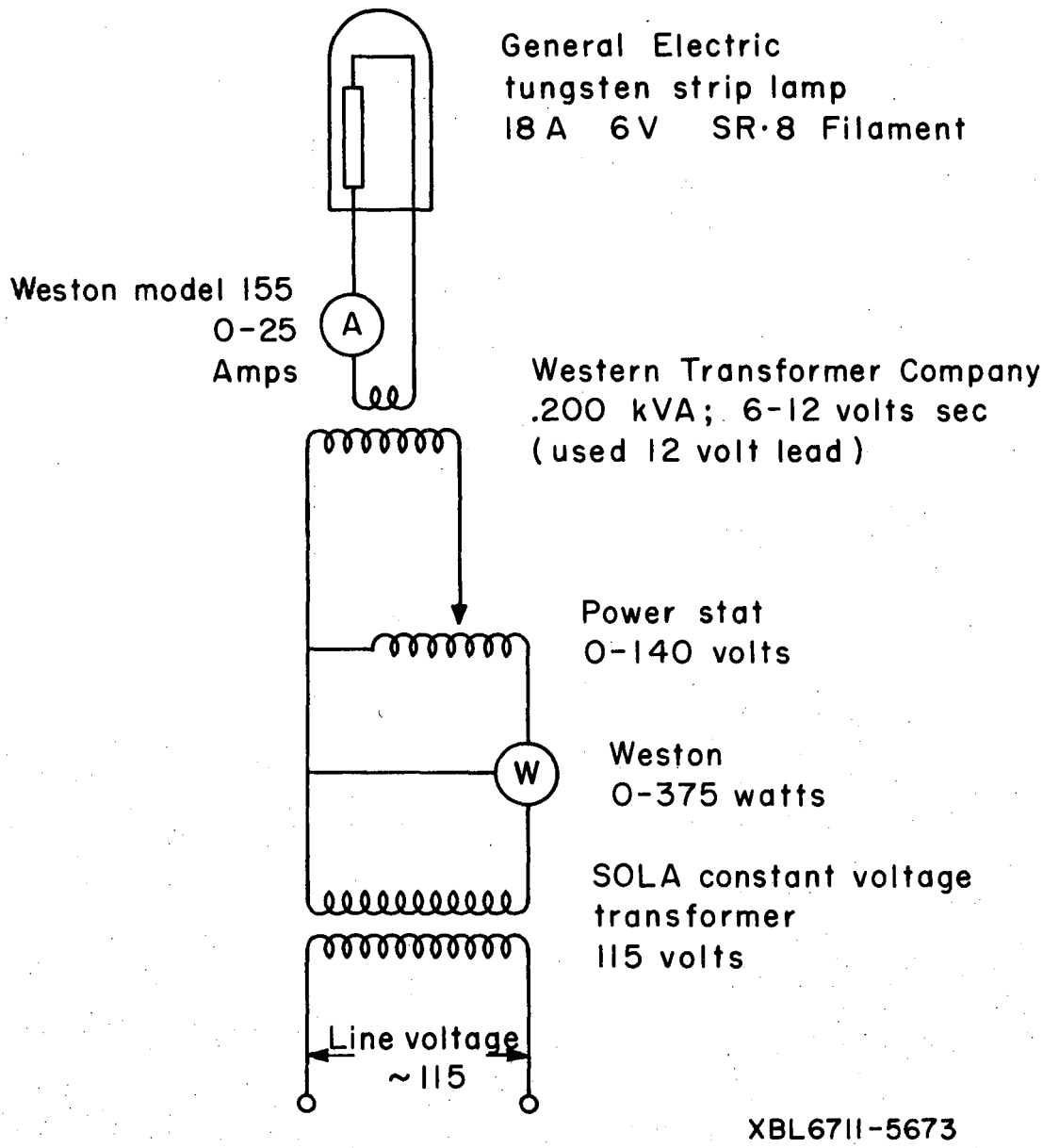

Fig. 7 Wiring diagram for the tungsten strip lamp.

because it resulted in sufficient absorption by ScF in the furnace and this power was used throughout this study. The measured current to the lamp was 20.85 amperes with variations less than .1 with different lamps and with the same lamp in different experiments.

Emission experiments used the same optics as absorption experiments, thus geometrical errors were avoided in comparison. Temperature could be measured during the course of an experiment through the window used previously for the absorption lamp. It was shown that temperature variations with time were small and at no time greater than 20° during the course of several exposures.

Thermal equilibrium could be reached within ten minutes or less, but normally at least fifteen minutes of warm-up time were allows. Reproducible temperature measurements before beginning exposures assured thermal equilibration.

Chromatic abberations in some lenses used gave slightly different focal points for the wavelengths studied. This resulted in large variations of relative intensities upon small variations in lens positions. This problem was eliminated by trial and error tests of many different lenses and optical arrangements. The final errors from this source were negligible.

The purpose of these studies in the King furnace was to relate observed equilibrium relative ScF electronic transition intensities to those of the molecular beam. In order to avoid errors due to the reciprocity effect of photographic plates, exposure times of the same order of magnitude were required. Neutral density filters were calibrated with a

Cary double beam spectrometer throughout the visible spectral region. In particular, the differences in density at the two wavelengths of interest were recorded. These filters were then put in the optical path before the iris diaphragm so that exposure times of three minutes could be used.

There is an apparent intensity difference at the singlet wavelength (5115 Å) and the triplet wavelength (6558 Å) from the differences in the sensitivity of the photographic plate and the differences in blackbody intensity. Experimentally the triplet becomes over-exposed at about the same exposure that the singlet approaches the linear region of the characteristic curve. Three methods were used to make intensity comparisons possible at the two wavelengths. By putting a 1.0 neutral density filter in the optical path on alternate exposures, the singlet and triplet wavelengths could be compared. In a series of thirteen exposures on a plate, compensation could be made for material losses by taking suitable averages. This method gave reasonable results, but because it is subject to several errors resulting from the exposures being made at different times, it was not the most satisfactory. Next a Corning color glass filter 4-97 or a Wratten 38 was used outside the Steinheil slit. Calibration of the Corning filter showed it to have a difference in transmission at the two wavelengths of interest equivalent to a density of 1.26 at the triplet wavelength; the Wratten filter was equivalent to a density of .81 at the triplet wavelength. Some exposures employed this procedure, but the rapid variation of transmission as a function of wavelength in the red caused background light interpretation problems. The most satisfactory method employed a 1.0 neutral density filter which was physically placed inside

the Steinheil in front of the photographic plate such that it covered only the red region of the spectrum. In this manner simultaneous measurements could be taken at both wavelengths.

A series of ScF absorption exposures were taken on a plate at a measured furnace temperature of 2100°C. The same exposure time of three minutes was used for all exposures while different calibrated neutral density filters from .1 to .9 were used to vary the exposure. Similarly a series of emission exposures were obtained either within the same experiment or entirely independently. The tungsten strip lamp through the identical geometry was used to obtain both the characteristic curves at the two wavelengths and the measured relative intensity of the lamp.

C. Molecular Beam

The molecular beam apparatus was first used by Walsh[46,47] for work of this type. His beam work on gaseous lanthanum monoxide[46] was repeated. Substantial modifications of the apparatus were required for this work due to the differences in vapor properties of ScF and those of LaO.

The stable room-temperature fluoride of scandium is ScF_3. Calculations based on estimates[48] of the thermodynamic properties of the fluorides of scandium indicate that ScF_3 is the principal vapor species even in the presence of scandium metal. Furthermore, ScF_2 is also an important vapor component. However, the percentage composition of the vapor changes such that ScF becomes a more important constituent as the temperature is increased.

It was found using the unmodified molecular beam apparatus that all the ScF_3 vaporized and the electronic spectrum of ScF was not observed. A double crucible arrangement was developed which would allow control of

the total vapor pressure at one temperature and the vapor composition at a second higher temperature.

Figures 8 and 9 show the shape of the crucible used. The other details of these two figures will be explained throughout the following text.

In order to prevent leaks due to non-uniform expansion from thermal gradients, the crucible was machined from one piece of tantalum 2.5 cm in diameter and 8.0 cm in length. The top portion of the container was 2.5 cm in both length and diameter with a wall thickness of about 1 mm. The bottom portion was 1.25 cm in diameter and 5.5 cm in length with a wall thickness of about 2 mm. An extension of about 1.0 cm of the bottom portion went into the top. Thus, liquid scandium could be held in the top part of the crucible at the higher temperature. The cap of the crucible was .62 cm thick with a circular orifice one mm in diameter.

In experiments ScF_3 powder of greater than 99.9% purity from Semi-Elements Inc., D. S. Goldsmith Chemical or Research Chemicals was placed in the lower portion of the crucible. Circles of .01 cm thick tantalum foil were fitted into the region directly above the ScF_3. These pieces of foil were easily removable for replacement of ScF_3. This portion of the crucible acted as a Knudsen cell with the leaks around the foil serving as orifices. Scandium metal of greater than 99.9% purity from Research Chemicals, Atomergic Chemetals Company or Bram Metallurgical was placed in the top part of the crucible.

A large temperature gradient was achieved using this double crucible. In early experiments a Pt vs Pt/10% Rh thermocouple was used to measure temperatures at the bottom of the crucible. With the top at 2100°C, the thermocouple read about 1000°C so the crucible barrel probably averaged

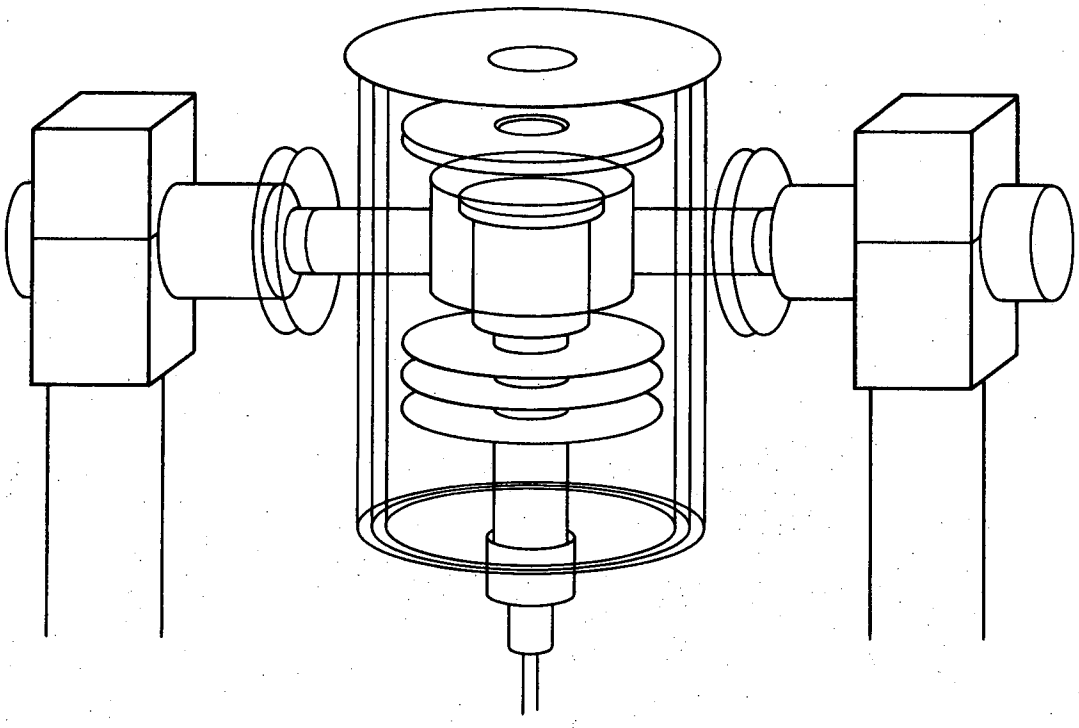

XBL6711-5717

Fig. 8 The molecular beam heating assembly with radiation shields.

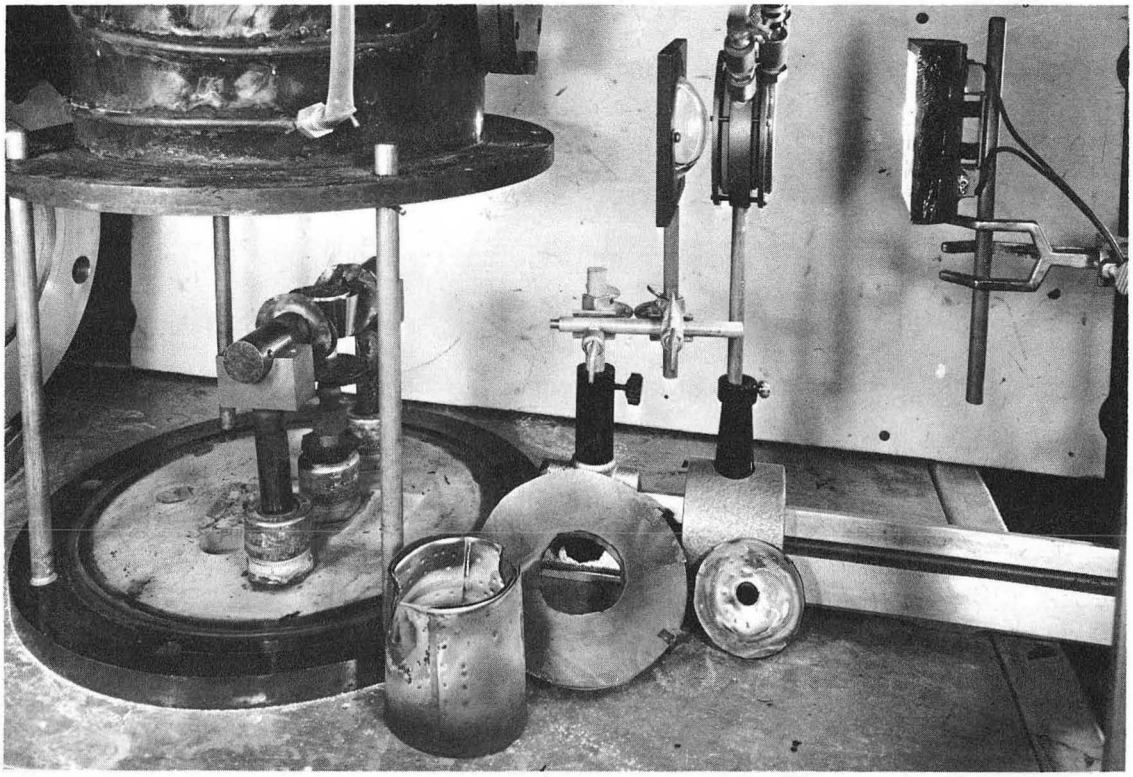

XBB 6711-6666

Fig. 9 The molecular beam crucible with resistance heating element.

about 1300°C. No convenient method was available to get accurate measurements except at the base of the crucible which means the effective temperature of the ScF_3 can only be estimated.

The molecular beam chamber was evacuated with a 15 cm diffusion pump, NRC model HS6-1500, type 162. A Kinney KC-15 mechanical pump served as both the roughing pump and fore-pump. A liquid nitrogen cold trap was located between the chamber and the diffusion pump. A background pressure of less than 5×10^{-6} torr could be obtained at room temperature. In normal operation, at least twelve hours of pumping at elevated temperatures were required to reach these background pressures.

Power was drawn from a single phase 208 volt source with 30 ampere fuses. A 7.8 KVA Superior Electric Company powerstat type 1256C controlled power input and an Electro Engineering Works 20 KVA, 41.5:1 type E11824 step-down transformer determined the current drawn by the heating element. A safety interlock system completed the circuit when adequate water flow was passing through the electrodes for cooling purposes. Two number 00 welding cables carried the current to each of the electrodes. Two identical pieces of .0125 cm thick tungsten foil 2.5 cm in height and 15 cm in length formed the resistance heating element. As shown in Figs. 8 and 9, these pieces of foil were shaped into concentric touching cylinders and attached to 1.25 cm diameter tantalum rod with small force-fitted tantalum tacks. The tantalum rod was fitted into a 2.5 cm diameter molybdenum rod. This in turn was attached to the water-cooled copper electrodes with a copper screw-on clamp. In operation, between 25 and 30 amperes were drawn at a voltage of about 250 volts from the source supply after passage through the variable transformer. So at the heating element about 1200 amperes were being passed and greater than 6 KVA of power was being dissipated.

Extensive heat radiation shielding was required to make optimum use of the power available. Figures 8 and 9 show part of the shielding used. Tantalum foil .01 cm thick was the material employed since it is easily formed and has sufficient structural strength at the operating temperatures. In contrast to the tungsten heating element which became very brittle after one experiment, the tantalum radiation shields could be used for many experiments. Close spacing of the shields was possible by dimpling the foil thus allowing only point contact with adjacent shields. In addition to those tantalum shields shown in Fig. 8, liberal use was made of graphite felt. The entire assembly including the electrodes was covered with a graphite felt rectangular box containing a circular opening for the molecular beam.

The crucible was supported by a connecting piece of tantalum to a molybdenum rod. A water cooled copper connection as well as the water-cooled electrodes were all 1.9 cm in diameter and were sealed with Crouse and Hinds number 396 rubber seals to provide simultaneous vacuum seals and electrical insulation. All three vacuum inlets were adjustable so that different molecular beam path lengths could be employed with only minor adjustments.

Figure 10 shows a schematic diagram of the optical path of the molecular beam system as viewed from the top of the beam chamber. The light source was a General Electric 120 volt, 650 watt movieflood DWY lamp. The filament was a tungsten coil with iodine vapor inside the quartz envelope. The lamp was operated on 110 volt AC power in an aluminum shield from a variable transformer.

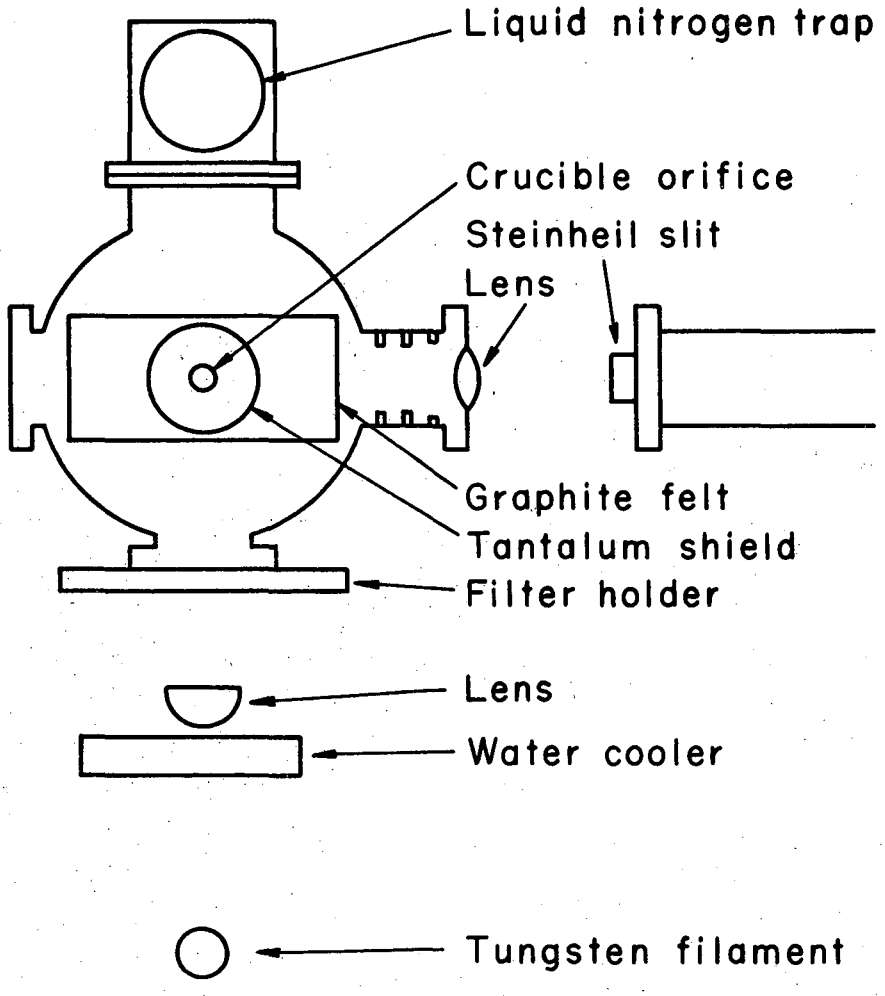

Fig. 10 Optical system for the molecular beam.

The water cooler which contained heat absorbing glass protected the lenses and filters by removing infrared radiation. A 7.5 cm focal length lens focused the image of the filament through the filter and chamber entrance window to a point directly over the beam orifice.

Corning color glass filter 3-72 was used to prevent excitation of wavelengths shorter than that of the singlet transition. In this manner cascading effects can be avoided. The combined effect of this filter and the heat absorbing glass was equivalent to a neutral density filter of .31 at the triplet wavelength.

Fluorescence was observed at right angles to the exciting light. A 9.7 cm focal length lens focused the fluorescence onto the Steinheil slit. Optical alighment was attained by placing a mirror above the crucible orifice. The lamp filament was focused onto the mirror and then the Steinheil was positioned such that the filament image was on its slit. The filament was 15.0 cm from the lens and approximately 24.5 cm from the entrance window. The Steinheil slit was about 11.2 cm from the lens on the exit window.

Temperature measurement was done with the same optical pyrometer used in the King furnace work. A glass prism on the cover of the molecular beam chamber allowed a line of sight directly into the crucible. With this method no corrections for emissivity of the crucible were applied since the cell should approach blackbody conditions. Corrections were applied for the prism.

The slit width, prism positions and other Steinheil adjustments were identical to those used during King furnace exposures. A 1.0 neutral density filter inside the Steinheil adjusted the light levels so that both the singlet and triplet wavelengths could be viewed simultaneously.

In a typical experiment the background pressure rose to approximately 1×10^{-4} torr where the mean free path for ScF in air is the order of 100 cm. The temperature inside the crucible was 2080 to 2100°C and 25 to 30 amperes were drawn from the source. Twelve minute exposures were taken. All the experimental details varied from experiment to experiment so that comparisons between any two different experiments are invalid, but there is little effect of these variations on the relative ScF fluorescent intensity.

D. Photographic Methods

Kodak 3-1/4 by 4-1/4 inch 103a-F photographic plates were used. Their spectral sensitivity is nearly identical at the two wavelengths studied. There is a sharp red cut-off beginning at about 6700 Å. The photographic speed was experimentally determined to be comparable to the Polaroid type 57 packets.

A constant temperature water bath was maintained at 20°C within .2°. Kodak D-19 developer, Hunt safety acid stop and Kodak Rapid Fixer were kept in 1.5 gallon stainless steel tanks in the bath. The acid stop was used to rapidly terminate development at four minutes. After ten seconds the plate was put in the fixer bath for five minutes. Then the plates were washed for at least thirty minutes.

Optical density measurements were performed with a Baird-Atomic Inc. model CB densitometer and were recorded on a Bristol model 560 strip chart recorder. The instrument allows measurement of densities from zero to 2.0. Experimentally the density recorded is a function of focus and the choice of zero density. Although these factors are small their effect upon weak features could result in unnecessary experimental uncertainties.

Averages were taken of several independent readings until the density was certain to .02 density units. It should be noted that the graininess of the photographic emulsion caused an uncertainty of .01 units.

Characteristic curves obtained with the cadmium atomic lines at 5086 and 6438 Å from an Osram lamp operated at 1.5 amperes proved subject to large Eberhard effects. These curves were unsuitable for photometric work. In principle, the ScF emission features could be employed to obtain characteristic curves. Material losses during the course of required exposure times and furnace instabilities make this method inaccurate. The tungsten strip lamp was used as the light source using the geometry of Fig. 6. Since the ScF features are subject to the Eberhard effect to some degree, this curve is a source of error when interpreting ScF features. Constant exposure times were used while varying the exposure with neutral density filters which were calibrated to give their true density as a function of wavelength. The characteristic curve was then plotted as the optical density measured from the densitometer against a relative log I scale. Figure 3 shows the experimental characteristic curve for the triplet wavelength for the photographic plates used. The characteristic curve for the singlet wavelength is nearly identical in appearance with a different log I scale.

V. RESULTS

A. Methods of Interpreting Experimental Data

From Eqs. (14) and (16) it can be seen that the beam fluorescence can be related to either absorption or emission in the King furnace. Experimentally the King furnace absorption and emission are compared through R_α by using Eq. (14) and R_α is then used to calculate expected beam intensities. It was found that emission intensities are more easily measurable so absorption was used as a check on the R_α values obtained from emission studies.

There is a background from the King furnace walls as well as scattering by optical components and dust in the furnace. Because this scattering can not be entirely eliminated and because its variation from experiment to experiment is in part uncontrollable, its interpretation is critical. The photographic response of the plate depends upon the total light intensity reaching it including both emission and background. The measurable densities are the peak density at the feature, D_p, and the estimated background density, D_b, chosen at the violet edge of the $^3\phi$-$^3\Delta$ violet-most (0,0) band head and at the minimum between the $^1\Pi$-$^1\Sigma^+$ (0,0) and (0,1) band heads.

From the tungsten lamp the shape of the characteristic curves are known at each wavelength. The value of I_{em} at each wavelength is of interest and can be obtained by converting from D_p and D_b to I_p and I_b in these two sets of relative units. It is known that

$$I_p = I_b + I_{em}. \tag{19}$$

So from the two observed densities and from the known characteristic curves for each wavelength

$$\begin{aligned} I_{em} &= I_p - I_b \\ &= 10^{\log I(D_p)} - 10^{\log I(D_b)}. \end{aligned} \tag{20}$$

log $I(D_p)$ is the value of log I at the density D_p and similarly for log $I(D_b)$.

The blackbody intensity in quanta per second per square centimeter normal to the source per unit solid angle per unit wavelength interval (in centimeters) is given by the following form of the Planck equation.

$$I = \frac{2c}{\lambda^4} \exp\left[\left(\frac{hc}{\lambda kT}\right)^{-1}\right]^{-1} \qquad (21)$$

The intensity ratio of a blackbody at T_g to a lamp at T_ℓ may be calculated from Eq. (21) by including the emissivity of the lamp filament. The one in Eq. (21) has been neglected.

$$\frac{I(\lambda)_{\text{lamp},T_\ell}}{I(\lambda)_{BB,T_g}} = \epsilon(T_\ell,\lambda) \exp\left[-\frac{hc\,(T_g - T_\ell)}{\lambda\, k\, T_g\, T_\ell}\right] \qquad (22)$$

The temperature of the previously described tungsten strip lamp filament was measured with the calibrated optical pyrometer. Three independent trials were made for a power level of 215 watts. The agreement between trials was as good as the agreement of measurements within one trial. This is experimental proof of ability to duplicate lamp conditions. The measured lamp temperature was 2587°C with an average error of 6°. The experimental pyrometer correction was such that the brightness temperature of this lamp is 2566°C or 2839°K at the wavelength of observation with the pyrometer (~6500 Å). Assuming a 92% transmission factor for the glass shield of the strip lamp[49] the true temperature of the lamp may be calculated.

$$\frac{1}{T_B} - \frac{1}{T} = -\frac{\lambda}{c_2} \ln\left[\tau, \epsilon(\lambda,T)\right] \qquad (23)$$

T is the true temperature, T_B the brightness temperature, λ the wavelength of observation, c_2 the second radiation constant, τ the transmission factor for the glass and ϵ the emissivity. Values for the emissivity of a tungsten strip lamp have been reported[50] as a function of the true temperature at various wavelengths. Extrapolation was required for the temperatures used in this work, but the errors should be negligible. The true temperature of the tungsten strip lamp is estimated to be 3235°K with an error of 10°.

For this lamp temperature and a blackbody at 2373°K (the King furnace and molecular beam operating temperature), Eqs. (22) and (12) may be combined to give the working equation for determining R_α from King furnace emission.

$$\alpha(\text{singlet}) = 10.31 \frac{I(s)_{em,KF,2373}}{I(s)_{lamp,3235}} \quad \text{and}$$

$$\alpha(\text{triplet}) = 4.88 \frac{I(t)_{em,KF,2373}}{I(t)_{lamp,3235}} \quad \text{or}$$

$$R_\alpha = .473 \frac{R_{em,KF,2373}}{R_{lamp,3235}} \tag{24}$$

In absorption studies in the King furnace the observables are the density due to the lamp, D_ℓ (chosen in the same manner that D_b was chosen in emission work), and D_p which is the optical density at the peak of the absorption feature. From these two densities, I_{abs}^{net} may be obtained in a manner analogous to that used to get I_{em} from Eq. (20). In order to calculate α, Eqs. (8), (10) and (11) are used to correct for that part of I_{abs}^{net} due to emission.

$$\frac{I^{net}_{abs,T_g}}{I_{lamp,T_\ell}} = \frac{I^{lamp}_{abs,T_g} - I_{em,T_g}}{I_{lamp,T_\ell}}$$

$$= \frac{\alpha I_{lamp,T_\ell} - \alpha I_{BB,T_g}}{I_{lamp,T_\ell}}$$

$$= \alpha \left[1 - \frac{I_{BB,T_g}}{I_{lamp,T_\ell}} \right] \qquad (25)$$

Applying the calculation used in Eqs. (22) and (24) at these temperatures the working equation for determining R_α from King furnace absorption studies is derived.

$$\frac{I^{net}_{abs,2373}}{I_{lamp,3235}} = .905\ \alpha(\text{singlet})$$

$$= .795\ \alpha(\text{triplet}) \quad \text{or}$$

$$R_\alpha = .878\ \frac{R^{net}_{abs,KF,2373}}{R_{lamp,3235}} \qquad (26)$$

This shows emission makes a substantial contribution to the observed optical density on the plate even though the lamp temperature is 862° greater than the gas temperature.

By the use of Eqs. (24) and (26) the King furnace emission studies are now comparable to the absorption studies.

The units of an intensity have no absolute meaning since the characteristic curves were plotted on an arbitrary log I scale. This means that all intensities obtained from these curves have unknown absolute values and, most importantly, the log I scales for the two wavelength regions are unrelated. In order to predict the ScF singlet intensity from that of the triplet in the molecular beam the log I scales must be related. The true intensity may be obtained at each wavelength by multiplying by a constant or by adding a constant to log I.

$$\begin{aligned} \log I(\text{triplet}) &= \log I(\text{triplet})_m + k \\ \log I(\text{singlet}) &= \log I(\text{singlet})_m + k \end{aligned} \tag{27}$$

The subscript m denotes the measured value obtained from the measured optical density and the characteristic curve. It should be noted that these constants include the photographic plate sensitivity.

The true value of R_α may be obtained from the measured values by applying Eq. (27) to Eq. (14) which relates the true intensities.

$$\begin{aligned} R_\alpha = \frac{R^{\text{lamp}}_{\text{abs},T_g}}{R_{\text{lamp},T_\ell}} &= \frac{I(t)^{\text{lamp}}_{\text{abs},T_g}}{I(s)^{\text{lamp}}_{\text{abs},T_g}} \times \frac{I(s)_{\text{lamp},T_\ell}}{I(t)_{\text{lamp},T_\ell}} \\ &= \frac{I(t)^{\text{lamp}}_{\text{abs},T_g,m}\ 10^{k}}{I(s)^{\text{lamp}}_{\text{abs},T_g,m}\ 10^{k'}} \times \frac{I(s)_{\text{lamp},T_\ell,m}\ 10^{k'}}{I(t)_{\text{lamp},T_\ell,m}\ 10^{k}} \\ &= \frac{R^{\text{lamp}}_{\text{abs},T_g,m}}{R_{\text{lamp},T_\ell,m}} \end{aligned} \tag{28}$$

A similar procedure shows R_α obtained from measured emission results gives the true R_α. In order to apply Eq. (16) to the experimental results the scales must be related. This can be done with the tungsten strip lamp since the relative intensity may be calculated as well as measured from the aribtrarily chosen log I scales. By applying Eq. (27) we get

$$\log R_{\text{lamp},T_\ell} = \log I(t)_{\text{lamp},T_\ell,m} + k - \log I(s)_{\text{lamp},T_\ell,m} - k' . \tag{29}$$

Using the Planck equation as expressed in Eq. (21) for the experimental conditions used in this study, the value of R_{lamp,T_ℓ} may be calculated.

$$R_{\text{lamp},T_\ell} = \left[\frac{\lambda(t)}{\lambda(s)}\right]^4 \frac{\epsilon(t)}{\epsilon(s)} \exp\left[\frac{hc}{kT_\ell} \frac{(\lambda(t) - \lambda(s))}{\lambda(t)\,\lambda(s)}\right]$$

$$= .3702 \frac{\epsilon(t)}{\epsilon(s)} \exp\left[\frac{6.190\times10^3}{T_\ell}\right] \tag{30}$$

By using the measured lamp temperature the two scales may now be related.

$$k - k' = .38 - \log R_{\text{lamp},3235,m} \tag{31}$$

In order to apply Eq. (16) to the experimental data from the molecular beam, one more quantity needs to be evaluated. R_{ex} may be found graphically from the paper of Studer and Van Beers[51] to be 2.3 in relative number of quanta or log R_{ex} is .36. The experimentally determined value is .39 with an average error from five numbers of less than .01. The experimental value is used in the following calculations.

Taking logs of both sides of Eq. (16) which is in true units and applying Eq. (27) to convert to the measured units we get

$$k' + \log I(s)_{f,B,T_g} = k + \log I(t)_{f,B,T_g} - \log R_\alpha R_{ex}. \qquad (32)$$

By applying Eqs. (28) and (29), Eq. (32) may now be written in the working form in terms of measured quantities.

$$\log I(s)_{f,B,2373} = \log I(t)_{f,B,2373} - \log R_\alpha - \log R_{lamp,3235} - .01 \qquad (33)$$

It should be noted that this equation does not include the correction term for fluorescence discussed in relation to Eq. (16) or the correction for the filter and water cooler employed of .31.

B. King Furnace

Table IV gives the experimentally determined values of $\log R_{lamp,3235}$. All densities are the average of five or more densitometer tracings. The values of log I are those taken from the arbitrary scales of characteristic curves with corrections applied for the neutral density filters used. Within a given plate (the same number with a different letter in the exposure number), the singlet or triplet intensity should be constant. The average of these 43 values gives $\log R_{lamp,3235}$ as 1.21 with an average error of .01.

The value of $\log R_\alpha$ was obtained from the experimental $\log R_{em}$ by applying Eq. (24) and using the experimental values of $\log R_{lamp,3235}$. Table V gives a summary of the data after densitometer readings were averaged and corrections for the neutral density filters were applied.

Table IV. Experimental values of log $R_{lamp,3235}$

Exposure Number	6558 Å Density	Corrected log I(t)	5115 Å Density	Corrected log I(s)	Measured log R_{lamp}
4-28- I-A	1.52	3.21	1.90	2.00	1.21
-B	1.09	3.23	1.45	2.00	1.23
-C	.98	3.21	1.40	2.01	1.20
-D	.71	3.20	1.16	2.01	1.19
-E	.28	3.21	.54	2.01	1.20
-F	.25	3.22	.46	2.01	1.21
-G	.15	3.22	.30	2.01	1.21
-H	.09	3.21	.19	2.00	1.21
-I	.09	3.26	.14	1.99	1.27
4-28- II-C	1.44	3.49	1.78	2.27	1.22
-D	1.15	3.50	1.49	2.27	1.23
-E	.80	3.49	1.23	2.29	1.20
-F	.71	3.49	1.12	2.30	1.19
-G	.46	3.51	.79	2.28	1.23
-H	.30	3.51	.55	2.30	1.21
-I	.25	3.51	.43	2.29	1.22
-J	.11	3.49	.22	2.29	1.20
-K	.06	3.49	.12	2.28	1.21
4-28-III-B	1.54	3.40	1.88	2.18	1.22
-C	1.28	3.43	1.55	2.18	1.23
-D	.61	3.41	1.03	2.21	1.20
-E	.34	3.43	.61	2.20	1.23
-F	.22	3.42	.40	2.21	1.21
-G	.17	3.41	.32	2.20	1.21
-H	.09	3.40	.21	2.20	1.20
-I	.06	3.44	.12	2.22	1.19
4-28- IV-A	1.52	3.19	1.90	2.00	1.19
-B	.70	3.18	1.14	2.00	1.18
-C	.29	3.20	.54	2.01	1.19
-D	.15	3.20	.30	2.01	1.19
-E	.08	3.22	.15	2.00	1.21
4-28- V-B	.89	3.26	1.31	2.08	1.18
-C	.58	3.26	1.04	2.08	1.18
-D	.36	3.26	.67	2.06	1.20
-E	.33	3.28	.55	2.06	1.22
-F	.20	3.27	.37	2.07	1.20
-G	.10	3.27	.21	2.08	1.19
-H	1.34	3.25	1.74	2.03	1.22
-I	.06	3.24	.13	2.00	1.24
-J	.91	3.25	1.36	2.04	1.21
-K	.17	3.23	.34	2.00	1.23
-L	.49	3.24	.82	1.99	1.25
-M	.31	3.25	.57	2.02	1.23
				Average	1.21±.01

Table V. Experimental values of log R_α from emission studies.

Exposure Number	Method Used*	Observed log $R_{em,2373}$	Calculated log R_α
4-45- I-K	1	1.42	-.12
4-45- IV-C	3	1.29	-.25
-D	3	1.26	-.28
-E	3	1.29	-.25
-F	3	1.35	-.19
-G	3	1.37	-.17
-H	3	1.38	-.16
-I	3	1.38	-.16
-J	3	1.50	-.04
-K	3	1.47	-.07
-L	3	1.43	-.11
-M	3	1.49	-.05
4-45- III-A	2	1.37	-.17
4-57- III-D	4	1.43	-.11
-E	4	1.45	-.09
-F	4	1.47	-.07
-G	4	1.47	-.07
-H	4	1.44	-.10
-I	4	1.47	-.07
-J	4	1.46	-.08
4-57- IV-B	3	1.43	-.11
-C	3	1.44	-.10
-D	3	1.42	-.12
-E	3	1.48	-.06
-F	3	1.50	-.04
-G	3	1.42	-.12
-H	3	1.41	-.13
-I	3	1.45	-.09
-J	3	1.47	-.07
		Average	-.12±.05

*1. A 1.0 neutral density used inside Steinheil.

2. A time average with no filters.

3. Corning 3-74 filter in front of exposures.

4. Wratten 38 filter in front of exposures.

The methods employed have been discussed previously in the text. The average was taken weighting exposure 4-45-III-A by four since four time average exposures were used. The average value of log R_α is -.12 with an average error of .05 for 32 values. There appears to be no systematic variation depending upon the method employed to reduce the triplet intensity to that of the singlet.

Equation (26) was combined with the experimental values of log $R_{lamp,3235}$ to obtain log R_α from the observed $R^{net}_{abs,KF,2373}$. Table VI summarizes the data. The average value for log R_α is -.04 with an average error of .08. This is in agreement with the value obtained from emission studies within experimental uncertainties. Since the absorption features are more difficult to measure and because the average error is larger, the value of log R_α from emission studies was used for further calculations.

C. Molecular Beam

Many trials were made with the molecular beam apparatus. Initial observation of the triplet ScF transition was made without filters. The data reported here were obtained with a 1.0 neutral density filter inside the Steinheil and using pre-exposed plates.

With the results of the King furnace work, Eq. (33) may be applied to predict the singlet fluorescent intensity from the measured triplet fluorescent intensity in the molecular beam.

$$\log I(s)_{f,B,2373} = \log I(t)_{f,B,2373} - 0.77. \qquad (34)$$

Table VII summarizes the data from three experiments with different molecular beam path lengths with average errors of measurement. The root mean square velocity of ScF in the beam at 2373°K was calculated from the

Table VI. Experimental values of log R_α from absorption studies.

Exposure Number	Method Used*	Observed log R_{abs}	Calculated log R_α
4-42- I-A	1	1.24	-.03
-B	1	1.27	.00
-C	1	1.33	.06
-D	1	1.03	-.24
-E	1	1.36	.09
-F	1	1.23	-.04
-G	1	1.16	-.11
-H	1	1.31	.04
4-45- I-D	1	1.16	-.11
-E	1	1.16	-.11
-F	1	1.34	.07
4-45-III	2	1.14	-.13
		Average	-.04±.08

*1. A 1.0 neutral density used inside Steinheil.
2. A time average with no filters.
3. Corning 3-74 filter in front of exposures.
4. Wratten 38 filter in front of exposures.

Table VII. $^1\Pi$-$^1\Sigma$ molecular beam fluorescent intensity.

Path Length (cm)	Transit Time (sec)	Calculated log I(s)	Observed log I(s)	Difference
9.2	8.2×10^{-5}	1.06± .03	.51 ± .03	.55 ± .06
10.2	9.2×10^{-5}	1.01± .02	.42 ± .02	.59 ± .04
11.8	1.1×10^{-4}	.97± .04	.34 ± .04	.63 ± .08

formula of Ramsey[52] to be 1.11×10^5 cm/sec. The transit time of ScF in the beam to the center of the entrance window was calculated using this number. All data in Table VII come from measurements of small optical density differences on photographic plates. An uncertainty of about .10 should be attached to the measured differences due to possible systematic errors. It should be noted that the columns of log I(s) are not comparable since they were obtained in independent experiments, but the differences are. The apparent change in the direction of $^1\Sigma$ to $^3\Delta$ decay is within experimental uncertainties. A lifetime of 1.5×10^{-4} seconds would produce a change of .09 units in log I over the extremes of path length employed.

Figure 11 shows a comparison of the absorption spectrum in the King furnace, the emission spectrum in the King furnace and the fluorescence spectrum in the molecular beam.

Self-absorption in emission studies and deviation from the linear curve of growth in absorption studies could be significant sources of error. The small ScF density in the molecular beam would give negligible errors from these sources. On the other hand, the King furnace studies are subject to large errors of this kind if the absorption or emission is

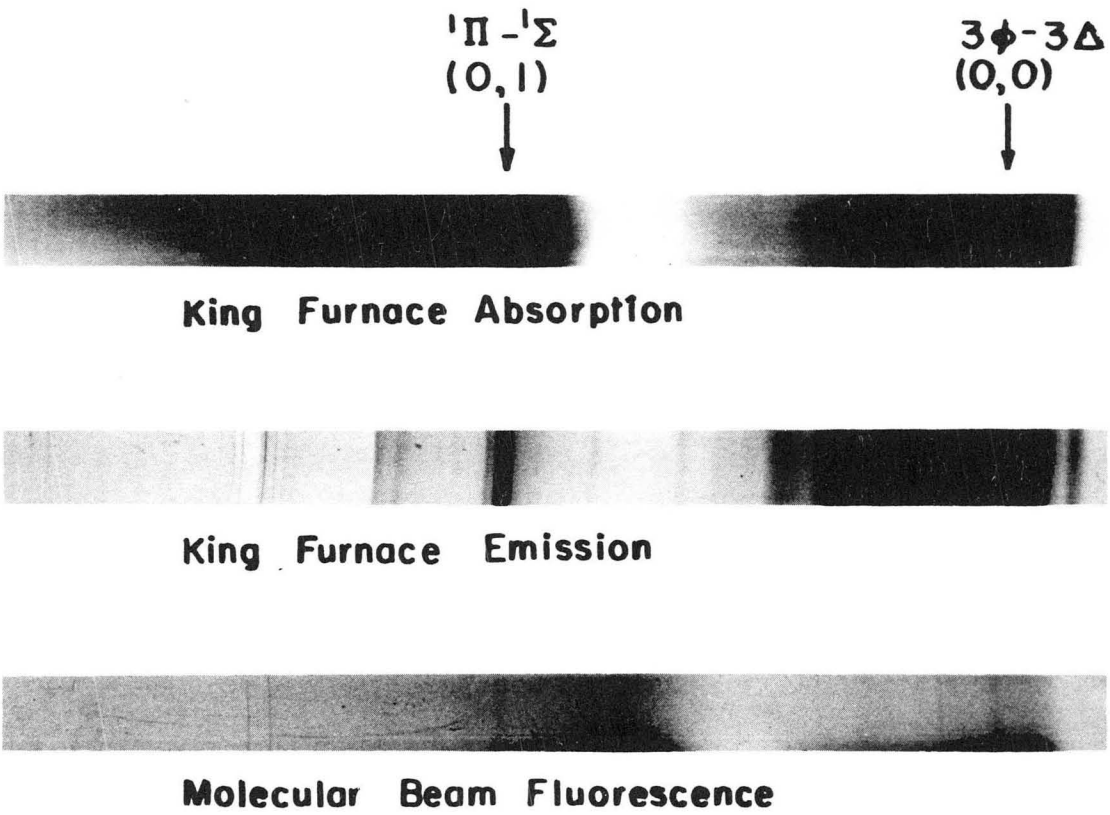

XBB 6712-6789

Fig. 11 Comparison of exposures of ScF.

strong. The apparent α values were estimated by calculating the spectrum of rotational lines near the observed heads from the known spectroscopic constants. By approximating the lines as triangles, the apparent spectrum and the true spectrum may be calculated as the sum of triangles. A computer program was written to add the intensities at intervals of 0.01 K using the Doppler width for the true spectrum and the instrumental width, calculated from the reciprocal dispersion and the slit width, for the observed spectrum. By comparison of the peak intensities, which were normalized to identical area triangles, the true α values may be inferred. Both true α values were less than 7%. This gives[53] a correction of about 0.2 to 0.3% due to self-absorption. Since interest in this work is in relative values, the net correction due to self-absorption or deviation from the linear curve of growth is negligible.

VI. DISCUSSION AND CONCLUSIONS

The molecular beam exposures demonstrate that both the $^1\Sigma^+$ and $^3\Delta$ states persist in the beam after a transit time of about 10^{-4} seconds. This places a lower limit on the lifetime of the higher energy of the two states of from 10^{-3} to 10^{-4} seconds. It would be possible within experimental uncertainties of about 25% to detect intensity variations with molecular beam path length for a lifetime in this range. The relationship among the f-value, lifetime (τ) and energy difference is well-known.[54]

$$f\,\tau = (mc/8\pi^2e^2)\,\frac{g_2}{g_1}\,\lambda_0^2 \qquad (35)$$

$$= 1.499\,\frac{g(^3\Delta)}{g(^1\Sigma)}\,\lambda_0^2$$

This formula is corrected from the reference for current values of the physical constants. λ_0 represents the wavelength of the transition in cm. It is assumed here that the $^1\Sigma^+$ is higher in energy than the $^3\Delta$ although analogous arguments apply if the reverse is the case. The lower and upper state degeneracies are represented by g_2 and g_1 respectively.

In Hund's case c where the selection rule $\Delta\Omega = 0, \pm 1$ applies, the transition $^1\Sigma^+ - {}^3\Delta_1$ would be allowed. The exposure shown in Fig. 11 was taken with the $^3\phi$-$^3\Delta$ intensity reduced by over a factor of ten and it does not show the three triplet heads clearly. Earlier exposures taken with no neutral density filter inside the Steinheil show that all three triplet heads appear in molecular beam fluorescence with roughly the same relative intensity as in the King furnace. The degeneracy of the $^3\Delta_1$ is two for the case c allowed transition. Equation (35) may then be written in terms of the energy separation, ΔE in kK, of the $^3\Delta$ and $^1\Sigma^+$ for this case.

$$\Delta E = (3.0 \times 10^{-6}/f\,\tau)^{1/2} \qquad (36)$$

A complete discussion of oscillator strengths or f-values for molecules is beyond the scope of this paper.[55] The strength of one rotational line is well-defined, but many measurements involve a band or sequence of bands. Franck-Condon factors must be accurately known. Experimental disagreements for atoms are common[54,56] and the data for molecules are sparse.[55] An estimate of the f-value for the $^1\Sigma^+ - ^3\Delta_1$ transition may be obtained by analogy to other molecules and a consideration of the coupling expected for ScF. The f-value of interest here is for an electronic transition as a whole including all vibronic transitions.

Table VIII lists combinations of assumed f-values with lifetimes of 10^{-4} and 10^{-3} seconds to give the energy limit of the $^1\Sigma^+$ above the $^3\Delta$. ΔE is obtained from Eq. (36) and represents an upper limit since only the lower limit of τ is known from the molecular beam fluorescence. Clearly the upper limit is very sensitive to the assumptions regarding f-values.

Table VIII. The energy separation of the $^3\Delta$ and $^1\Sigma^+$.

Assumed f-value	Assumed lifetime (sec)	Energy separation (kK)
10^{-2}	10^{-4}	1.7
10^{-3}	10^{-4}	5.5
10^{-4}	10^{-4}	17.0
10^{-5}	10^{-4}	55.0
10^{-2}	10^{-3}	.6
10^{-3}	10^{-3}	1.7
10^{-4}	10^{-3}	5.5
10^{-5}	10^{-3}	17.0

The f-value of the $B^3\Pi_{0u^+}$-$^1\Sigma_g^+$ transition of I_2 has been calculated from observed lifetimes[56] to be approximately 10^{-2} assuming a mean wavelength of 8000 Å. This would be the maximum f-value to be expected for ScF. An analysis of the mixing of states of different multiplicity in ScF has not been done, but it has been suggested that there are reasonably large effects.[15] It would seem that in view of the large number of observed and predicted low-lying electronic states that a high degree of configuration interaction should occur. This would give substantial "triplet character" to the singlets and vice-versa resulting in a high f-value for the intercombination transition.

It should be noted that additional symmetry restrictions in a homonuclear molecule like I_2 would prevent mixing of states which could mix in an isoelectronic heteronuclear molecule.[4] Thus I_2 may be too restrictive a case for determining what the upper limit of the f-value might be in ScF.

The degree to which a molecule approaches Hund's coupling case c from cases a or b may be estimated in part by its molecular weight.[4] Lighter diatomic molecules formed from second and third row elements have more and more evidence of case c character. The $^3\Pi$-$^1\Sigma$ transitions have been observed and analyzed in AlBr[56] and AlCl.[57] The molecular weight of AlCl is close to that of ScF and the molecules are somewhat analogous in electronic structure. The observation in this case of a forbidden transition is a strong indication that AlCl has a significant degree of case c coupling. The d-orbitals of Sc lead to a large number of low-lying atomic energy levels (see Fig. 2) which implies that ScF should have a much larger effect due to configuration interaction than AlCl. Thus, ScF should have an f-value considerably larger than that of AlCl.

An indication of case c character is the difference in spectroscopic of the case a multiplet sublevels.[59] In ScF the three rotational constants of the $^3\Delta$ differ by about two percent. This may be taken as an indication of departure of the coupling from case a.

Perhaps the strongest evidence for a strong ScF intercombination transition is the observed[60] absorption from the $^1\Sigma$ ground-state of GaF to both the Π and $^3\Pi$ states. This gives a direct indication of comparable transition probabilities to the "allowed" and "forbidden" states. The molecular weight of GaF is only slightly greater than that of ScF and there are similarities in bonding.

From the various possibilities listed in Table VIII, it is felt that a reasonable upper limit on the energy separation is about 3.0 kK. This estimate takes into account the available information indicating an f-value the order of 10^{-3}. The lifetime could be of the order of seconds, since only a limit has been established; in which case the energy separation is considerably less.

The partition function of gaseous ScF is probably best represented as a sum of contributions from three states at most temperatures. It is recommended on the basis of this work that the $^3\Delta$ and $^1\Delta$ be treated as degenerate for thermodynamic purposes. The unobserved $^1\Delta$ state is probably from .5 to 2.5 kK above the electronic ground state and its contribution to the partition function is important at most temperatures.

Table IX gives approximate spectroscopic constants for the three low-lying states of ScF. The values are calculated from the data of Barrow et al.[2] for the $^3\Delta$ and $^1\Sigma^+$ states. The constants for the $^1\Delta$ are estimated by comparison of the known $^1\Delta$ and $^3\Delta$ states of TiO and using the same

Table IX. Approximate spectroscopic constants for ScF.

	$^3\Delta$	$^1\Sigma^+$	$^1\Delta$
T_0 (kK)	0.0	0.0	2.0
ω_e (k)	648	736	650
$\omega_e x_e$ (k)	3.03	3.8	3.1
B_e (k)	.3623	.3950	.37
α_e (k)	.0025	.00266	.0026

percentage differences for ScF. The T_0 values are estimates based on this work. Table X gives the calculated free-energy function using standard formulas.[61] The harmonic oscillator approximation was used.

Table X. The free-energy function of gaseous scandium monofluoride (cal/deg/mole).

T(°K)	Translation	Rotation*	Vibration*	Electronic	$-\frac{F^\circ - H_0^\circ}{T}$
298	33.438	13.917	1.452	3.867	52.674
1000	39.433	16.376	2.300	3.899	62.008
1500	41.446	17.129	2.821	3.948	65.344
2000	42.876	17.748	3.249	3.997	67.870
2500	43.986	18.146	3.589	4.038	69.759
3000	44.890	18.506	3.892	4.074	71.362

* Includes contribution from both the $^3\Delta$ and $^1\Sigma^+$.

Relative absorption intensity in the molecular beam may be calculated from an equation similar to Eq. (34). The relative fluorescence intensity would be identical to that in absorption if all the light in the upper states fluoresced to the same energy level from which it was originally absorbed. In the molecular beam work account must be taken of the Franck-Condon factors from the initial state of fluorescence: the v = 0 levels of the $^1\Pi$ and $^3\phi$. The internuclear distance of v = 0 of the $^1\Sigma^+$, $^1\Pi$, $^3\Delta$ and $^3\phi$ states using the rotational constants of Barrow[2] are calculated to be 1.79, 1.87, 1.86 and 1.90 Å respectively. Since the change in internuclear distance for the singlet (0,0) transition is greater than that for the triplet (0,0), it would be expected that the $^3\phi$-$^3\Delta$ (0,0) transition would have the larger Franck-Condon factor. Furthermore it is estimated that the Franck-Condon factor for the $^3\phi$-$^3\Delta$ (0,0) transition should be larger than that for the $^1\Pi$-$^1\Sigma^+$ (0,1) since the v = 0 level of the $^1\Pi$ should have comparable overlap with several v". This would result in a calculated singlet fluorescent intensity based on the observed triplet fluorescent intensity which is larger than that which is observed. Table VII shows that this is the case. The singlet transition is less intense than calculated by about a factor of four. This seems to be a reasonable number to account for the expected Franck-Condon factors.

If there is an allowed electronic transition, further reduction of the fluorescent intensity from that expected is possible. Table III earlier in the text shows that there is an unobserved $^3\Pi$ state below the $^3\phi$. The transition $^3\phi$-$^3\Pi$ is forbidden[4] by the case a selection rule $\Delta\Lambda = 0, \pm 1$. In addition it would be at an energy which is unfavorable relative to the allowed $^3\phi$-$^3\Delta$ transition. Therefore, the $^3\phi$-$^3\Pi$ should take a very small

percentage of the light away from the $^3\phi$-$^3\Delta$. There are no other triplet transitions to be expected.

On the other hand, a $^1\Pi$-$^1\Delta$ transition is allowed and the unobserved $^1\Delta$ might be expected to be an important factor in the reduction of observed singlet fluorescent intensity from that calculated. This work shows that this is probably not the case. The $E^1\Pi$-$A^1\Delta$ is at most of comparable intensity and more likely weaker than the $E^1\Pi$-$X^1\Sigma^+$. In order to observe the $^1\Delta$ state, emission transitions involving other upper states must be found. Both the $C^1\Sigma^+$ and $B^1\Pi$ have allowed transitions with the $E^1\Pi$, but their wavelengths are less favorable. No effect was observed from these two states.

Discussions of experimental errors have been included at appropriate points within the text. The factor of four reduction in singlet fluorescence intensity from that calculated is felt to be accurate within twenty percent. It is difficult to place accuracy limits on the $^1\Sigma^+$-$^3\Delta$ energy separation since the assumptions involved with determining a suitable f-value are more uncertain than experimental errors.

As previously discussed, the corrections for self-absorption are less than one percent. Furthermore, the Boltzmann factors should be similar for the $^1\Sigma^+$ and $^3\Delta_1$ states because of the size of kT compared to the energy separation of the two states. The (0,0) R-head of the $^3\phi_2$-$^3\Delta_1$ occurs at about J = 28 and the (0,1) R-head of the $^1\Pi$-$^1\Sigma^+$ at about J = 12. Therefore, the experimental value of R_α represents a ratio of f_{abs} values within experimental uncertainties and the uncertainty of relative population. It may be concluded that the ratio of the $^3\phi$-$^3\Delta$ f_{abs} value to that of the $^1\Pi$-$^1\Sigma^+$ is 0.8±3.

Thermodynamically the partition function of gaseous scandium fluoride is better defined. Three electronic states make appreciable contributions. Spectroscopically it would be desirable to know better the exact location of these three states. The ScF spectrum is complex, but a careful analysis of the weaker features may show an intercombination transition which is capable of analysis. From the arguments presented, the f-value for the intercombinations should not be too much smaller than those for allowed transitions. An analysis of the emission spectrum of ScF should be undertaken to locate the unobserved $^1\Delta$ and $^3\Pi$ states. Perhaps an analysis of the observed[13] perturbations may reveal singlet-triplet interactions which would allow the relative energy of the $^3\Delta$ and $^1\Sigma^+$ states to be better defined.

ACKNOWLEDGMENTS

I am grateful to Professor Leo Brewer for both his ideas and his patience in explaining them. His inspiration and insight have been of great personal value as well as necessary for the completion of this work. I owe a great deal to members of his research group, both past and present, who have given helpful suggestions thoughout the course of this work.

I owe special thanks to my wife, Sally, whose confidence and encouragement helped me pass through some discouraging periods.

This work was performed under the auspices of the United States Atomic Energy Commission.

REFERENCES

1. Leo Brewer, Principles of High Temperature Chemistry in Proceedings of the Robert A. Welch Foundation Conferences on Chemical Research, (Robert A. Welch Foundation, Houston, Texas, 1962), pp. 47-92.
2. R. F. Barrow et al., Nature 215, 1072 (1967).
3. Albin Lagerqvist and Ulla Uhler, Arkiv For Fysik 1, 459 (1949).
4. Gerhard Herzberg, Spectra of Diatomic Molecules (D. Van Nostrand Co., Inc., Princeton, New Jersey, 1950).
5. E. A. Ballik and D. A. Ramsey, Astrophys. J. 137, 61 (1963).
6. E. A. Ballik and D. A. Ramsey, Astrophys. J. 137, 84 (1963).
7. John G. Phillips, Astrophys. J. 115, 567 (1952).
8. See for example, G. D. Brabson, Ph. D. Thesis, University of California, UCRL-11976, August 1965.
9. C. C. J. Roothaan, Rev. Mod. Phys. 23, 69 (1951).
10. See for example, Robert G. Paar, Quantum Theory of Molecular Electronic Structure, (W. A. Benjamin Inc., New York, 1964).
11. R. F. Barrow et al., Proc. Phys. Soc. 83, 889 (1964).
12. R. F. Barrow and W. J. M. Gissane, Proc. Phys. Soc. 84, 615 (1964).
13. R. F. Barrow, private communication.
14. Donald McLeod Jr., and William Weltner Jr., J. Phys. Chem. 70, 3293 (1966).
15. K. Douglas Carlson and Carl Moser, J. Chem. Phys. 46, 35 (1967).
16. R. T. Birge and A. Christy, Phys. Rev. 29, 212 (1927).
17. R. T. Birge and A. Christy, Nature 122, 205 (1928).
18. F. Lowater, Proc. Phys. Soc. 41, 557 (1929).
19. A. Christy, Phys. Rev. 33, 701 (1929).
20. K. Wurm and H. J. Meister, Z. Astrophys. 13, 199 (1936).

21. John G. Phillips, Astrophys. J. 111, 314 (1950).

22. John G. Phillips, Astrophys. J. 114, 152 (1951).

23. John G. Phillips, Astrophys. J. 119, 274 (1954).

24. U. Uhler, Dissertation, Stockholm (1954).

25. A. V. Pettersson, Naturwiss. 46, 200 (1959).

26. A. V. Petterson, Arkiv För Fysik 16, 185 (1959).

27. A. V. Pettersson and B. Lindgren, Naturwiss. 48, 128 (1961).

28. A. V. Pettersson and B. Lindgren, Arkiv För Fysik 22, 491 (1962).

29. K. Douglas Carlson, J. Chem. Phys. 67, 2644 (1963).

30. K. Douglas Carlson and R. K. Nesbit, J. Chem. Phys. 41, 1051 (1964).

31. W. Weltner and D. McLeod, J. Phys. Chem. 69, 3488 (1965).

32. I. Kovacs, J. Mol. Spect. 18, 229 (1965).

33. R. Toros, Acta Physica 20, 91 (1966).

34. A. Lagerqvist, U. Uhler and R. F. Barrow, Arkiv För Fysik 8, 281 (1954).

35. U. Uhler, Arkiv För Fysik 8, 295 (1954).

36. U. Uhler and L. Akerlind, Arkiv För Fysik 10, 431 (1955).

37. L. Akerlind, Arkiv För Fysik 11, 395 (1956).

38. W, Weltner and D. McLeod, Nature 206, 87 (1965).

39. C. E. Moore, National Bureau of Standards Circular 467 (1949).

40. C. E. Kenneth Mees, The Theory of the Photographic Process (Macmillian Co., New York, 1966), 3rd Edition.

41. T. H. James and George C. Higgins, Fundamentals of Photographic Theory, (John Wiley and Sons, Inc., New York, 1948).

42. L. Brewer, P. W. Gilles and F. A. Jenkins, J. Chem. Phys. 16, 797 (1948).

43. John L. Engelke, (Ph. D. Thesis), University of California, UCRL-8727 (April 1959).

44. Lucy G. Hagan, (Ph. D. Thesis), University of California, UCRL-10620 (March 1963).

45. Oscar H. Krikorian, (Ph. D. Thesis), University of California, UCRL-2888 (April 1955).

46. Robert M. Walsh, (Ph. D. Thesis), University of California, UCRL-11927 (April 1965).

47. Leo Brewer and Robert Walsh, J. Chem. Phys. 42, 4055 (1965).

48. Leo Brewer, L. A. Bromley, P. W. Gilles and N. L. Lofgren, The Thermodynamic Properties of the Halides, in Chemistry and Metallurgy of Miscellaneous Materials: Thermodynamics L. L. Quill, Editor (McGraw-Hill Book Co., Inc., New York, 1950).

49. G. A. W. Rutgers and J. C. De Vos, Physica 20, 715 (1954).

50. J. C. De Vos, Physica 20, 690 (1954).

51. F. J. Studer and R. F. Van Beers, J. Opt. Soc. Am. 54, 945 (1964).

52. Norman F. Ramsey, Molecular Beams (Oxford Press, London, 1956).

53. Leo Brewer, W. T. Hicks and O. H. Krikorian, J. Chem. Phys. 36, 182 (1962).

54. Allan C. G. Mitchell and Mark W. Zemansky, Resonance Radiation and Excited Atoms, (Cambridge Press, London, 1934).

55. J. B. Tatum, The Interpretation of Intensities in Diatomic Molecular Spectra, Astrophys. J. Suppl. Ser. XVI (124), 21 (1967).

56. Ara Chutjian, (Ph. D. Thesis), University of California, UCRL-16441 (Jan. 1966).

57. Devendra Sharma, Astrophys. J. 113, 219 (1951).

58. Devendra Sharma, Astrophys. J. 113, 210 (1951).

59. Robert S. Mulliken, Rev. Mod. Phys. 3, 89 (1931).

60. R. F. Barrow and D. Welti, Nature 168, 161 (1951).

61. G. N. Lewis and M. Randall, Rev. Kenneth S. Pitzer and Leo Brewer, Thermodynamics, 2nd Edition, (McGraw-Hill Book Co., Inc., New York, 1961).